Received: 7 June 2021 | Accepted: 17 January 2023

DOI: 10.1111/pce.14544

ORIGINAL ARTICLE

Plant, Cell & Environment | WILEY

Cation diffusion facilitator proteins of *Beta vulgaris* reveal diversity of metal handling in dicotyledons

Santiago Alejandro | Bastian Meier | Minh Thi Thanh Hoang | Edgar Peiter

Plant Nutrition Laboratory, Faculty of Natural Sciences III, Institute of Agricultural and Nutritional Sciences, Martin Luther University Halle-Wittenberg, Halle (Saale), Germany

Correspondence
Santiago Alejandro and Edgar Peiter, Plant Nutrition Laboratory, Faculty of Natural Sciences III, Institute of Agricultural and Nutritional Sciences, Martin Luther University Halle-Wittenberg, D-06099 Halle (Saale), Germany.
Email: santiago.alejandro-martinez@landw.uni-halle.de and edgar.peiter@landw.uni-halle.de

Funding information
Deutsche Forschungsgemeinschaft, Grant/Award Number: INST271/371-1 FUGG; European Regional Development Fund, Grant/Award Number: ZS/2016/06/79740; European Social Fund, Grant/Award Number: ZS/2016/08/80644

Abstract

Manganese (Mn), iron (Fe), and zinc (Zn) are essential for diverse processes in plants, but their availability is often limiting or excessive. Cation diffusion facilitator (CDF) proteins have been implicated in the allocation of those metals in plants, whereby most of our mechanistic understanding has been obtained in Arabidopsis. It is unclear to what extent this can be generalized to other dicots. We characterized all CDFs/metal tolerance proteins of sugar beet (*Beta vulgaris* spp. *vulgaris*), which is phylogenetically distant from Arabidopsis. Analysis of subcellular localization, substrate selectivities, and transcriptional regulation upon exposure to metal deficiencies and toxicities revealed unexpected deviations from their Arabidopsis counterparts. Localization and selectivity of some members were modulated by alternative splicing. Notably, unlike in Arabidopsis, Mn- and Zn-sequestrating members were not induced in Fe-deficient roots, pointing to differences in the Fe acquisition machinery. This was supported by low Zn and Mn accumulation under Fe deficiency and a strikingly increased Fe accumulation under Mn and Zn excess, coinciding with an induction of *BvIRT1*. High Zn load caused a massive upregulation of *Zn-BvMTPs*. The results suggest that the employment of the CDF toolbox is highly diverse amongst dicots, which questions the general applicability of metal homeostasis models derived from Arabidopsis.

KEYWORDS
deficiency, iron, manganese, metal tolerance protein, metal transport, sugar beet, toxicity, zinc

1 | INTRODUCTION

Various transition metals are essential for photosynthetic organisms. For instance, in the chloroplast, manganese (Mn) is an essential cofactor of the oxygen-evolving complex (OEC), which catalyzes the water-splitting reaction in photosystem II (PSII), iron (Fe) is integral to the photosynthetic electron transfer chain, and zinc (Zn) is necessary for the repair of PSII (Yruela, 2013). Furthermore, Fe, Zn, and copper (Cu) are cofactors of the Fe superoxide dismutase (FeSOD) and the CuZnSOD, respectively, which act as reactive oxygen species (ROS) scavengers in chloroplasts (Andresen et al., 2018). Fe is also required for biogenesis of Fe-S clusters, Fe-heme groups and di-iron centers in mitochondria, and it is a cofactor of the peroxisomal FeSOD (Corpas et al., 2017). On the other hand, Mn is essential for numerous Golgi-localized glycosyl transferases involved in protein glycosylation and biosynthesis of pectin and hemicellulose polymers, and it is also the cofactor of MnSOD in mitochondria and peroxisomes (He et al., 2022; He et al., 2021). However, when their concentrations in

cytosol or organelles are above the physiologically acceptable range, those metals may exert cellular damage and induce deficiencies of other metals (Andresen et al., 2018). Therefore, the uptake and intracellular distribution of the micronutrients must be tightly regulated to achieve optimum growth.

The availability of Mn and Fe may vary between limiting and excessive, as dependent on soil conditions. Mn is bioavailable to plants only in the reduced state (Mn^{2+}), but in soils with high organic matter content, high redox potential, or alkaline reaction, Mn^{2+} is rapidly oxidized, generating insoluble oxidation forms (Alejandro et al., 2020). Conversely, in acidic or waterlogged soils, soluble Mn concentrations may reach toxic levels. Fe availability is similarly dependent on soil pH and redox potential (Colombo et al., 2014). All plants except graminaceous monocots acquire Fe as Fe^{2+}, which is made available by the release of protons and Fe(III) chelators, and by a membrane-bound Fe(III) chelate reductase activity (Andresen et al., 2018). By contrast, Zn exhibits only one oxidation state (+2), its availability being low on calcareous soils (Cakmak, 2000).

Since Fe, Mn, and Zn deficiency are widespread plant nutritional disorders, adaptative responses to counter a short supply have been studied in the model plant species, *Arabidopsis thaliana* (Arabidopsis) and *Oryza sativa* (rice). Mechanisms to cope with the nutritional imbalances include the transcriptional regulation of specific transport proteins to control the uptake, translocation, and distribution of these micronutrients into the different subcellular compartments (Andresen et al., 2018). In particular, transcriptional responses to low Fe availability and the function of Fe deficiency-responsive genes have been extensively explored (Schwarz & Bauer, 2020). In contrast, the available information on transcriptional responses to low Mn or Zn availability is limited to few studies on Zn (Mager et al., 2018; Sinclair et al., 2018; van de Mortel et al., 2006) and Mn deficiency (Rodríguez-Celma et al., 2016; Yang et al., 2008).

Among the players involved in micronutrient distribution and homeostasis, members of the cation diffusion facilitator (CDF) family play crucial roles in bacteria, archae, and eukaryotes (Gustin et al., 2011). These transporters, called metal tolerance proteins (MTPs) in plants, have a wide range of divalent metal cation substrates, including Mn^{2+}, Fe^{2+}, and Zn^{2+}, which they generally transport out of the cytoplasm, either into subcellular compartments or the apoplast (Ricachenevsky et al., 2013). The proteins usually contain four to six transmembrane domains (TMDs) with cytoplasmic N- and C-termini (Kolaj-Robin et al., 2015). MTP family members in all kingdoms have been grouped into three clusters: Zn-MTP, Mn/Fe-MTP, and Fe/Zn-MTP, based on their confirmed or putative metal specificities (Eroglu et al., 2017; Montanini et al., 2007; Ricachenevsky et al., 2013). Fe/Zn-MTP proteins have been identified in different plant species, but their function and subcellular localization have not been determined yet. More information is available on Zn-MTPs and Mn/Fe-MTPs in plants. The Arabidopsis Zn-MTPs AtMTP1 and AtMTP3 are localized to the tonoplast and function in the vacuolar sequestration of excess Zn (Arrivault et al., 2006; Kobae et al., 2004). Thereby AtMTP3 is required to detoxify Zn in Fe-deficient plants, which overaccumulate Zn and Mn due to the activity of the poorly selective Fe transporter iron-regulated transporter1 (IRT1). In contrast, the endoplasmic reticulum (ER)-localized AtMTP2 is an important factor for Zn efficiency and suggested to promote symplastic Zn tunneling within the ER of root cells (Sinclair et al., 2018). Furthermore, it has been reported that AtMTP12 is part of a functional complex with AtMTP5 to transport Zn into the Golgi apparatus (Fujiwara et al., 2015). Mn/Fe-MTP transporters operate in the tonoplast and in diverse endomembranes (Alejandro et al., 2020; He et al., 2021). Arabidopsis AtMTP8 detoxifies Mn by sequestration in root vacuoles (Eroglu et al., 2016). As this process is particularly important in Fe-deficient Arabidopsis, *AtMTP8* is highly upregulated under Fe deficiency. This transporter is also pivotal in the accumulation of Mn in specific tissues of developing embryos and in the interim storage of Fe during germination (Eroglu et al., 2017; Höller et al., 2022). The rice orthologs OsMTP8.1 and OsMTP8.2 have also been characterized as transporters implicated in vacuolar Mn sequestration, albeit not related to the Fe deficiency response (Chen et al., 2013; Takemoto et al., 2017). In *Lupinus albus*, which mobilizes large amounts of Mn by P-starvation-induced root exudates, *LaMTP8* detoxifies Mn in leaf vacuoles (Olt et al., 2022). In contrast to the vacuolar MTP8 proteins, the barley orthologs HvMTP8.1 and HvMTP8.2 have been localized to the Golgi (Pedas et al., 2014). The closely related AtMTP9 and AtMTP10 were shown to transport Mn^{2+} in yeast, but their function and subcellular localization in plants have not been determined yet (Chu et al., 2017). However, the AtMTP9/10 ortholog in rice, OsMTP9, has been described as a plasma membrane-localized transporter implicated in root-to-shoot translocation of Mn (Ueno et al., 2015). Moreover, AtMTP11 has been localized to the Golgi apparatus, where it functions in the detoxification of excess Mn likely mediated by vesicular trafficking (Peiter et al., 2007). Transporters belonging to the MTP family have been characterized in other plant species, such as wheat, sweet orange, and grape (Fu et al., 2017; Shirazi et al., 2019; Vatansever et al., 2017). However, those studies are largely based on in silico analyses and mostly do not take into account physiological roles of the genes.

Physiological roles of dicot MTP transporters in the handling of Fe, Mn, and Zn have thus been analysed almost exclusively in Arabidopsis. It is unclear, if the functional models derived from these studies are universally valid for dicots in general. Such conservation would be fundamentally important for translational approaches employing our knowledge of Arabidopsis to improve micronutrient efficiency and metal tolerance of crops. We chose sugar beet (*Beta vulgaris* L ssp. *vulgaris*), a dicot that is phylogenetically distant to Arabidopsis, to explore this question. Sugar beet is a root crop which is agriculturally important because of its ability to accumulate high concentrations of sugar in the taproot. To date, sugar beet research has been targeted mainly at increasing yield and extractable sugar, as well as pathogen resistance (Monteiro et al., 2018). However, although sugar beet is prone to boron (B), Fe, Mn, and Zn deficiency in the field (Draycott, 2006), physiological

effects of low supply and the involvement of players known from Arabidopsis in responses to nutritional imbalances are largely obscure. Here, we characterize the impact of Fe, Mn, and Zn deficiency on photosynthesis and nutrient homeostasis of sugar beet, and assess the involvement of MTP proteins under those conditions. This analysis revealed that localization, regulation, and hence physiological roles, of some family members differ markedly from those in Arabidopsis, indicating a greater heterogeneity in transition metal handling in the plant kingdom as previously assumed.

2 | MATERIALS AND METHODS

2.1 | Identification and sequence analysis of *MTP* genes and proteins in sugar beet

To identify MTP homologs in *B. vulgaris*, all 12 AtMTP amino acid sequences were used as query sequences in BLASTP searches of the KWS2320 sugar beet protein sequence RefBeet-1.2 (http://bvseq.molgen.mpg.de/blast/) with a cut-off E-value of $1e^{-5}$. All obtained sequences were sorted as unique sequences for further cation efflux protein domain search using InterProScan Sequence Search (http://www.ebi.ac.uk/Tools/pfa/iprscan/). The molecular weight (MW) and isoelectric point (pI) of the MTP proteins were calculated using ExPASy (http://web.expasy.org/compute_pi/). The gene code, splice variants, and chromosomal positions of the genes were obtained from the sugar beet genome database BeetSet_2 (https://jbrowse.cebitec.uni-bielefeld.de/RefBeet1.5) and the NCBI *Beta vulgaris* subsp. *vulgaris* Annotation Release 100 database (https://www.ncbi.nlm.nih.gov/genome/annotation_euk/Beta_vulgaris_subsp._vulgaris/100/). The transmembrane domains of the proteins were assessed by using Phobius (http://phobius.sbc.su.se/), and the transit peptides were predicted by using TargetP 1.1 (http://www.cbs.dtu.dk/services/TargetP/). Gene structure analysis was performed by GSDS 2.0 (http://gsds.cbi.pku.edu.cn/). Multiple sequence alignment was performed with ClustalW (https://embnet.vital-it.ch/software/ClustalW.html) and drawn in Genedoc (http://genedoc.software.informer.com/).

2.2 | Phylogenetic analyses and sequence alignments

Phylogenetic trees were constructed from ClustalW-aligned full-length proteins by MEGA7.0 (http://www.megasoftware.net/history.php) using the neighbor-joining (NJ) method, with 1000 bootstrap replicates with pairwise deletion option for handling alignment gaps, and with the Poisson correction model for distance computation (homogeneous substitution pattern among lineages), to infer phylogeny on all lineages, since several pairwise distances could not be assigned with the equal input correction mode. BvMTPs were named based on the phylogenetic analysis and sequence homology with Arabidopsis MTP proteins.

2.3 | Plant material and growth conditions

Sugar beet seeds (KWS2320) were germinated on wet filter paper at 16°C in darkness for 6 days. Then, the hypocotyl of seedlings was inserted into a sliced polyethylene foam plug, and 40 seedlings were placed into a 1 L container filled with hydroponic solution composed of 1.3 mM KNO_3, 1 mM $Ca(NO_3)_2$, 0.4 mM $MgSO_4$, 0.26 mM NH_4NO_3, 0.2 mM KH_2PO_4, 25 µM Fe-EDTA, 19 µM H_3BO_3, 10 µM $MgCl_2$, 5 µM $MnSO_4$, 0.3 µM $ZnSO_4$, 0.13 µM $CuSO_4$, and 0.05 µM MoO_3. The pH of the solution was adjusted to 5.5 with KOH. Media was aerated with atmospheric air controlled by a flow-meter (Cole-Parmer). Hydroponic trays were placed in a plant growth cabinet (VB 1014, Vötsch) set to 23°C/19°C day/night cycle and a 16-h light period (300 µmol m^{-2} s^{-1}) for 9 days to allow further growth. For micronutrient deficiency treatments, eight seedlings were transferred to a 4.5-L container filled with aerated hydroponic solution with no added Fe-EDTA (−Fe), $MnSO_4$ (−Mn), or $ZnSO_4$ (−Zn), and those grown in hydroponic solution containing all nutrients were used as control. For metal excess treatments, sugar beet seedlings were grown for 17 days before treatment. Solutions were changed every 7 days. Photosynthetic activity, gene expression levels, chlorophyll, and element concentrations were measured in the youngest fully developed leaves.

For hydroponic experiments with Arabidopsis, seeds were sown on ½ MS vertical plates and placed in the growth cabinet used for sugar beet set to 23°C/19°C day/night cycle and a 16-h light period (100 µmol m^{-2} s^{-1}). Then, seedlings were inserted into a sliced polyethylene foam plug, and 15 seedlings were placed into a 4.5-L container filled with the hydroponic solution described above. For plate experiments, Arabidopsis seeds were grown on ½ MS vertical plates at 21°C/19°C and a 16-h light period (100 µmol m^{-2} s^{-1}).

2.4 | Measurements of chlorophyll and photosynthetic parameters

A chlorophyll meter (SPAD-502Plus, Konica-Minolta) was used to take SPAD values from two fully expanded young leaves on each plant. A total of four plants were measured for each growth condition, and three SPAD values per leaf were averaged as the mean SPAD value of the leaf. An Imaging Pulse-Amplitude-Modulation (PAM) chlorophyll fluorometer and the software ImagingWIN version 2.47 (both Heinz Walz) were employed to determine photosynthetic parameters. Before the experiment, plants were dark-adapted for 30 min. Fluorescence measurements of young detached leaves were recorded by illumination for 2 s with 3000 µmol photons m^{-2} s^{-1} at a wavelength of 650 nm. PSII maximum efficiency (F_v/F_m) and F_o were calculated from the recorded fluorescence parameters. The experiment was replicated with comparable results.

2.5 | Mineral element analyses

Roots and young leaves of plants were separated. Leaves were rinsed with deionized water and dried at 70°C. Roots were washed in cold 1 mM MES (pH 5.7) for 10 min, then rinsed with deionized water, washed in cold 10 mM EGTA, 1 mM MES (pH 5.7) for 10 min, and dried at 70°C. Dry leaves and roots were weighed into polytetrafluoroethylene (PTFE) tubes and digested in a solution of HNO_3, H_2O_2, and ultrapure water (3:1:1) using a microwave digester (Mars 5 Xpress, CEM). Elemental analysis was performed using microwave plasma-atomic emission spectrometry (4210 MP-AES, Agilent). The experiments were replicated with comparable results.

2.6 | RNA extraction and quantitative reverse transcription polymerase chain reaction (qRT-PCR) analysis

Total RNA was isolated from young leaves and roots using a Spectrum™ Plant Total RNA kit (Sigma-Aldrich). Then, first strand complementary DNA (cDNA) was synthesized using M-MuLV Reverse Transcriptase (New England Biolabs) according to the manufacturer's protocol. PCR reactions were conducted on a MasterCycler ep RealPlex^4 S system (Eppendorf) using a final volume of 10 µL containing 5 µL PerfeCTa SYBR Green Supermix Reagent (Quantabio), 1 µL of cDNA, and 0.2 µM gene-specific primers (Supporting Information: Table S1). The PCR reaction conditions were 95°C for 30 s, followed by 40 cycles of 95°C for 30 s, 55°C for 30 s, and 72°C for 25 s. The relative expression levels were normalized by using the average of three housekeeping genes (*BvACT7*, *BvEF1*, *BvGAPDH* for sugar beet and *AtACT2*, *AtTUB6*, and *AtUBQ10* for Arabidopsis) as reference values. The comparative C_t ($2^{-\Delta\Delta C_t}$) method was applied for quantification. Three technical replicates were performed for each qRT-PCR reaction. The experiments were replicated with comparable results.

2.7 | Yeast complementation

Sequences encoding *BvMTPs*, *BvIRTs*, and *AtMTP1* were PCR-amplified from sugar beet and Arabidopsis cDNA by using gene-specific primers (Supporting Information: Table S1), and inserted by the USER cloning reaction into a USER-compatible modified pFL61 vector (Nour-Eldin et al., 2006). The pFL61-AtMTP8 construct was described previously (Eroglu et al., 2016). The pFL61-MTP constructs were then transformed into the *Saccharomyces cerevisiae* yeast strains Δ*zrc1* (Y00829), Δ*ccc1* (Y04169), and Δ*pmr1* (Y04534). The pFL61-BvIRT constructs were transformed into the yeast mutants Δ*fet3*Δ*fet4* (DDY4) and Δ*smf1* (Y06272). The pFL61 empty vector was used as a negative control, and the wild type strain BY4741 (Y00000) harboring pFL61 was used as positive control. In the case of the Δ*fet3*Δ*fet4* mutant, the DY150 strain was used as wild type. Cultures of each yeast strain containing one of the genes of interest were grown in liquid SC-URA medium. Then 10-µL aliquots of each yeast culture at optical densities (OD_{600}) of 1.0, 0.1, and 0.01 were spotted onto the respective restrictive media. The experiments were replicated with comparable results.

2.8 | Subcellular localization

To determine the subcellular localization of sugar beet and Arabidopsis MTP proteins, the coding region of *BvMTP* and *AtMTP1* genes were amplified with the gene-specific primers shown in Supporting Information: Table S1. These CDS sequences were cloned by the USER cloning reaction into a USER-compatible modified pART7 vector in-frame with an mCherry tag in the C-terminus. In the case of *AtMTP1*, an EGFP tag was used. Constructs were transiently expressed in freshly isolated protoplasts from 3- to 4-week-old sugar beet seedlings or 4- to 5-week-old Arabidopsis plants, as previously described (Peiter et al., 2007). After transformation, protoplasts were observed with a confocal laser scanning microscope (LSM 880 Airyscan, Carl Zeiss) equipped with a Plan-apochromatic lens (×63/1.4 Oil). The pART7-AtMTP8-GFP construct was obtained by amplification of *AtMTP8* from pART7:MTP8 (Eroglu et al., 2016) and cloning into the pART7:mGFP5 vector (Peiter et al., 2007). A vector derived from pFGC5941 carrying the first 29 amino acids of cytochrome c oxidase IV from *S. cerevisiae* fused to GFP (Nelson et al., 2007) was used as mitochondrial marker. The ER marker consisted of a combination of the signal peptide of AtWAK2 at the N-terminus of GFP and the ER retention signal His-Asp-Glu-Leu at its C-terminus (Nelson et al., 2007).

2.9 | Transgenic Arabidopsis lines

A cassette including the 35S promoter, the coding region of the *BvMTP* genes, and the 3′ocs terminator was subcloned from pART7-BvMTP1, pART7-BvMTP11α, and pART7-BvMTP11β into the pBART vector (Peiter et al., 2007) by *NotI* digestion. Constructs were transformed in *Agrobacterium tumefaciens* GV3101 by electroporation, and Arabidopsis mutants *ozs1* (Weber et al., 2013) and *mtp11-1* (Peiter et al., 2007) were transformed by the floral-dip method (Clough & Bent, 1998). The resulting seeds were selected by BASTA, and the T2 generation was used for further analyses.

3 | RESULTS

3.1 | Identification and classification of *MTP* genes in sugar beet

To identify sugar beet *MTP* genes, a BLASTP search on the *Beta vulgaris* resource database was performed using the 12 MTP proteins

TABLE 1 Summary of the sugar beet *BvMTP* gene family.

Name	Gene code	Amino Acids	MW (kDa)	pI	TMD	Transit peptide	Sustrate (this work)	Localization (this work)
BvMTP1	Bv1_002330_xpwe	419	46.0	6.1	6	-	Zn	Vesicles (in *B.v.*) tonoplast (in *A.t.*)
BvMTP4	Bv7_188800_eexc	356	39.9	6.1	6	-	-	Endomembrane
BvMTP5	Bv3_066040_qndu	400	44.8	8.6	6	Chloroplast	-	Chloroplast
BvMTP6	Bv7_178970_wncp	504	55.5	6.7	5	-	-	Endomembrane
BvMTP7α	Bv7_193680_mnog	452	50.0	6.5	6	Mitochondria	-	
BvMTP7β	Bv7_193680_mnog	456	50.6	6.6	6	Mitochondria	-	Mitochondria
BvMTP8.1	Bv3_075740_ryth	417	47.0	5.3	6	-	Fe, Mn	Tonoplast
BvMTP8.2	Bv4_078380_yiwe	402	45.5	5.5	6	-	Fe, Mn	Endomembrane
BvMTP9α	Bv1_023100_scux	378	43.7	7.7	6	-	Mn	Endomembrane
BvMTP9β	Bv1_023100_scux	401	46.2	6.3	6	-	Fe, Mn	Endomembrane
BvMTP11α	Bv2_040710_ecai	408	45.9	4.9	6	-	Mn	Tonoplast
BvMTP11β	Bv2_040710_ecai	351	39.7	4.9	6	-	Mn	Golgi
BvMTP12	Bv3_055170_rawz	873	98.7	6.6	16	-	-	ER

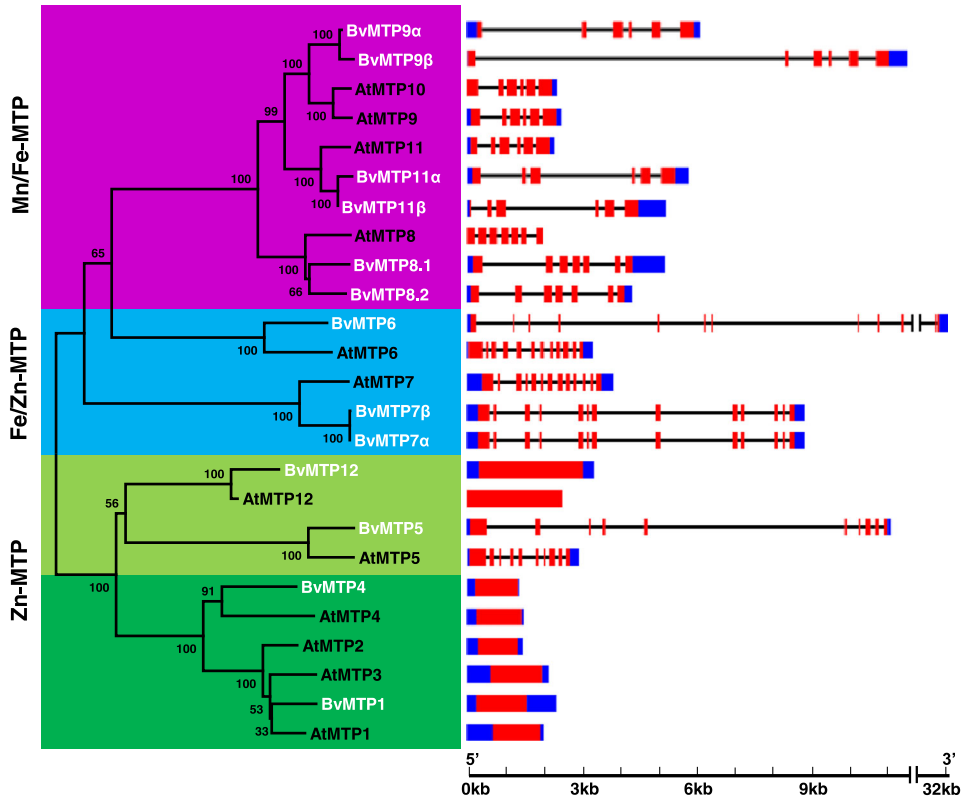

FIGURE 1 Phylogeny and intron–exon structure of *MTP* genes of *Arabidopsis thaliana* and sugar beet (*Beta vulgaris*). BvMTP and AtMTP proteins were used to construct the neighbor-joining tree. Blue boxes, red boxes, and black lines represent untranslated regions, exons, and introns, respectively, and their lengths are shown proportionally. The Zn-MTP proteins are divided into two subgroups according to their phylogenetic relationships.

from *Arabidopsis thaliana* as queries. After a validation to confirm the presence of a cation efflux protein domain, 10 *BvMTP* genes were identified (Table 1). A second analysis using the NCBI sugar beet database revealed that three *BvMTPs* have two splice variants, denoted as α and β, as result of alternative start codons. A phylogenetic analysis of Arabidopsis and sugar beet MTP proteins was performed to systematically classify them, and BvMTPs were named according to their similarity to AtMTPs (Figure 1). The

phylogenetic tree shows that BvMTP8.1, BvMTP8.2, BvMTP9α/β, and BvMTP11α/β belong to the Mn/Fe-MTP cluster; BvMTP6 and BvMTP7α/β to the Fe/Zn-MTP cluster; and BvMTP1, BvMTP4, BvMTP5, and BvMTP12 to the Zn-MTP cluster. The exon-intron organization is conserved between Arabidopsis and sugar beet *MTP* genes. However, exons are more widely dispersed with larger introns in *BvMTP* genes as compared to *AtMTPs*. In particular, the *BvMTP6* gene has a length of 32 kb. The *BvMTP* genes are distributed across five of the nine sugar beet chromosomes (Supporting Information: Figure S1) with no *BvMTP* genes located close to each other. It is therefore suggested that no tandem duplication events occurred in the evolutionary history of sugar beet *MTP* genes.

3.2 | Sequence analysis of BvMTP proteins

BvMTP proteins are predicted to have 5-6 TMDs, with a length ranging from 356 to 504 amino acids, and molecular masses from 39.9 to 55.5 kDa (Table 1). As exception, BvMTP12 as the largest member of the family has approximately twice the number of amino acids and putative TMDs compared to other sugar beet MTPs. BvMTP7β is four amino acids (MQWR) longer than BvMTP7α, whereas the amino acid sequences of BvMTP9 and BvMTP11 splice variants differ in the N-terminal region (Supporting Information: Figure S2). These splice variants were confirmed by PCR-amplification from cDNA using specific primers and sequencing. Interestingly, BvMTP5 and BvMTP7α/β have a predicted chloroplastic and mitochondrial transit peptide, respectively. Since the *BvMTP7* splice variants only differ in four amino acids in the N-terminal region, it was not possible to design specific primers for qRT-PCR analyses of the *BvMTP7* splice variants.

An alignment of AtMTP and BvMTP sequences showed that Zn-MTPs are conserved with the exception of At/BvMTP5, which are more divergent in the TMD region and contain a shorter cytosolic loop between TMD IV and V (Supporting Information: Figure S3a). The Zn-MTP cluster can generally be discerned by the presence of two consensus motifs, HxxxD (x = any amino acid), and a histidine/serine-rich (H/S) region between TMD IV and V (Montanini et al., 2007). Here, both consensus motifs as well as the H/S region are present in most Zn-MTPs, except for MTP5 of both species.

Proteins of the sugar beet Mn/Fe-MTP subfamily have highly conserved sequences (Supporting Information: Figure S3b). All of them contain the two DxxxD consensus motifs specific for this subgroup (Montanini et al., 2007). By contrast, members of the plant Fe/Zn cluster exhibit a high degree of sequence divergence with no specific domains or conserved residues (Gustin et al., 2011; Ricachenevsky et al., 2013). Therefore, BvMTP6 and BvMTP7 were independently aligned with their respective closest homologs from Arabidopsis (Supporting Information: Figure S4). This alignment analysis shows a high degree of conservation in TMDs, but not in N-termini.

3.3 | *BvMTP* genes complement yeast mutants defective in Fe, Mn, and Zn transport

The in silico analyses indicated a high degree of conservation of the MTP family in Arabidopsis and sugar beet, with some notable differences, such as a duplication of MTP8, and less Mn/Fe-MTPs and Zn-MTPs in sugar beet. This provoked the question whether their substrate specificity is conserved. To determine the proteins' selectivities, the *BvMTP* genes were expressed in yeast mutants defective in vacuolar sequestration of Fe (Δ*ccc1*) and Zn (Δ*zrc1*), and in the loading of Golgi vesicles with Mn (Δ*pmr1*). In the presence of 1 mM $MnSO_4$, the growth defect of Δ*pmr1* cells was abolished by all *Mn/Fe-MTP* genes and splice variants, that is, *BvMTP8.1*, *BvMTP8.2*, *BvMTP9α/β*, and *BvMTP11α/β* (Figure 2). This is in agreement with an analysis of two Mn/Fe-MTPs that were described as Mn transporters in the sugar beet relative *Beta vulgaris* spp. *maritima* (Erbasol et al., 2013). On medium containing 10 mM $FeSO_4$, only *BvMTP8.1*, *BvMTP8.2*, and *BvMTP9β* rescued the growth of Δ*ccc1*. Interestingly, the splice variant *BvMTP9α* was unable to do so, indicating an essential function of the N-terminus in the discrimination of Mn versus Fe by BvMTP9 (Figure 2). Finally, only *BvMTP1* was able to complement the Δ*zrc1* mutant on medium containing 15 mM $ZnSO_4$. As Arabidopsis AtMTP8 and AtMTP1 have been described as Fe/Mn and Zn transporters, respectively, these proteins were used as positive controls in yeast complementation assays (Supporting Information: Figure S5).

The in silico analysis showed that BvMTP5 and BvMTP7β harbor a putative chloroplastic and mitochondrial transit peptide, respectively. Since this may interfere with their transport activity, the yeast mutants were transformed with a truncated version of those genes, devoid of the transit peptide. However, neither $BvMTP5^{\Delta 1-61}$ nor $BvMTP7^{\Delta 1-100}$ was able to rescue any of the yeast strains (Supporting Information: Figure S6).

Taken together, these results suggest that all members of the sugar beet Mn/Fe-MTP cluster transport Mn. A subset of those has the ability to transport Fe, whereas only one sugar beet MTP transports Zn in our assays. The transported substrate of a number of BvMTPs, including all of the Fe/Zn subgroup, remains obscure.

3.4 | *BvMTP1* and *BvMTP11α/β* complement the metal sensitivities of Arabidopsis *mtp1* and *mtp11* mutants

Arabidopsis *AtMTP1* and *AtMTP11* are well-characterized Zn and Mn transporters, respectively. To further analyse if their sugar beet counterparts share these substrates, as indicated by the yeast complementation assays (Figure 2), *BvMTP1* and *BvMTP11α/β* were stably expressed in Arabidopsis knockout mutants. Heterologous expression of rice *OsMTP1* in Arabidopsis has previously been shown to rescue Zn sensitivity of a *mtp1*

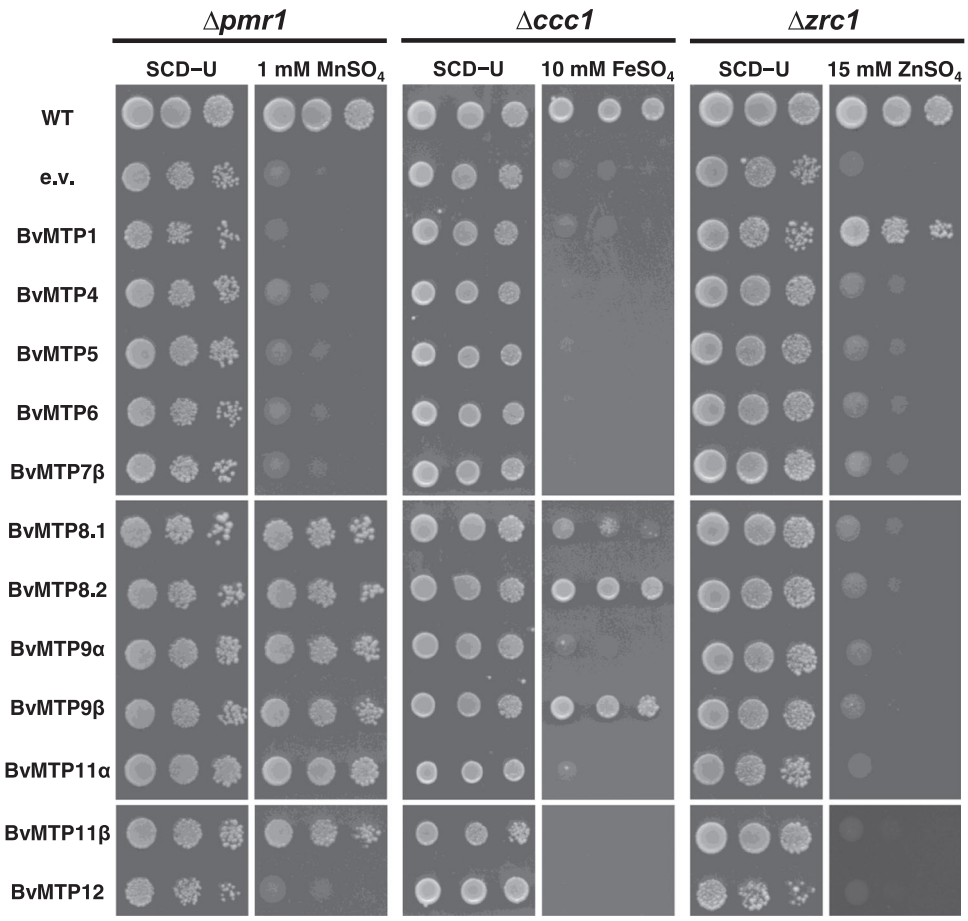

FIGURE 2 *BvMTP* genes complement yeast strains sensitive to Mn, Fe, and Zn. *Δpmr1*, *Δccc1*, and *Δzrc1* yeast mutants were transformed with the pFL61 empty vector (e.v.), or with pFL61 containing *BvMTPs*. Yeast cells were grown on selective media (SC−Ura) with metal supplementation as indicated. Precultured cells were diluted to an OD_{600} of 1.0, 0.1, and 0.01, and spotted onto plates. Plates were incubated for 72 h at 30°C.

mutant (Menguer et al., 2013), consistent with the function of MTP1 in the transport of Zn into the vacuole for sequestration. To define the function of BvMTP1 *in planta*, an Arabidopsis *AtMTP1* loss-of-function allele, *ozs1* (Weber et al., 2013), was stably transformed with *BvMTP1* under the control of a constitutive 35S promoter. The *ozs1* mutant is sensitive to elevated Zn, suffering stunted growth and reduced fresh weight compared with the wild type (Figure 3a). The tolerance to high Zn was restored when *ozs1* was transformed with *BvMTP1*. In addition, we examined whether sugar beet BvMTP11*α/β* function *in planta* as Mn transporters, like their Arabidopsis homolog, AtMTP11, which plays a role in the detoxification of excess Mn (Peiter et al., 2007). This was explored by expressing *BvMTP11α/β* in the Arabidopsis *mtp11-1* mutant, which has previously been shown to display reduced shoot weight and root growth rate compared to wild type under high Mn load (Peiter et al., 2007). Stable expression of both *BvMTP11* splice variants clearly rescued the Mn-hypersensitive phenotype of *mtp11-1* (Figure 3b,c).

The results substantiate the notion that BvMTP1 and BvMTP11*α/β* function as transporters for Zn and Mn, respectively, and mediate the detoxification of those metals, as their Arabidopsis homologs.

3.5 | BvMTP proteins localize to diverse subcellular compartments

The substrate selectivities of BvMTPs resembled those of their Arabidopsis counterparts, with a notable reduction of Zn-transporting members to only one. We next queried the locations of their operation. In Arabidopsis, MTPs operate in a range of organelles, including the vacuole, ER, and vesicular compartments, with known functions in these membranes. To determine the subcellular localization of BvMTPs, we chose to avoid heterologous expression, and transiently expressed *BvMTP-mCherry* fusions in sugar beet mesophyll protoplasts. Microscopic observations revealed that BvMTPs were all localized in various endomembranes (Supporting Information: Figure S7 and Table 1).

To get a closer insight into the subcellular localization, some *BvMTP* fusions were coexpressed with subcellular markers and

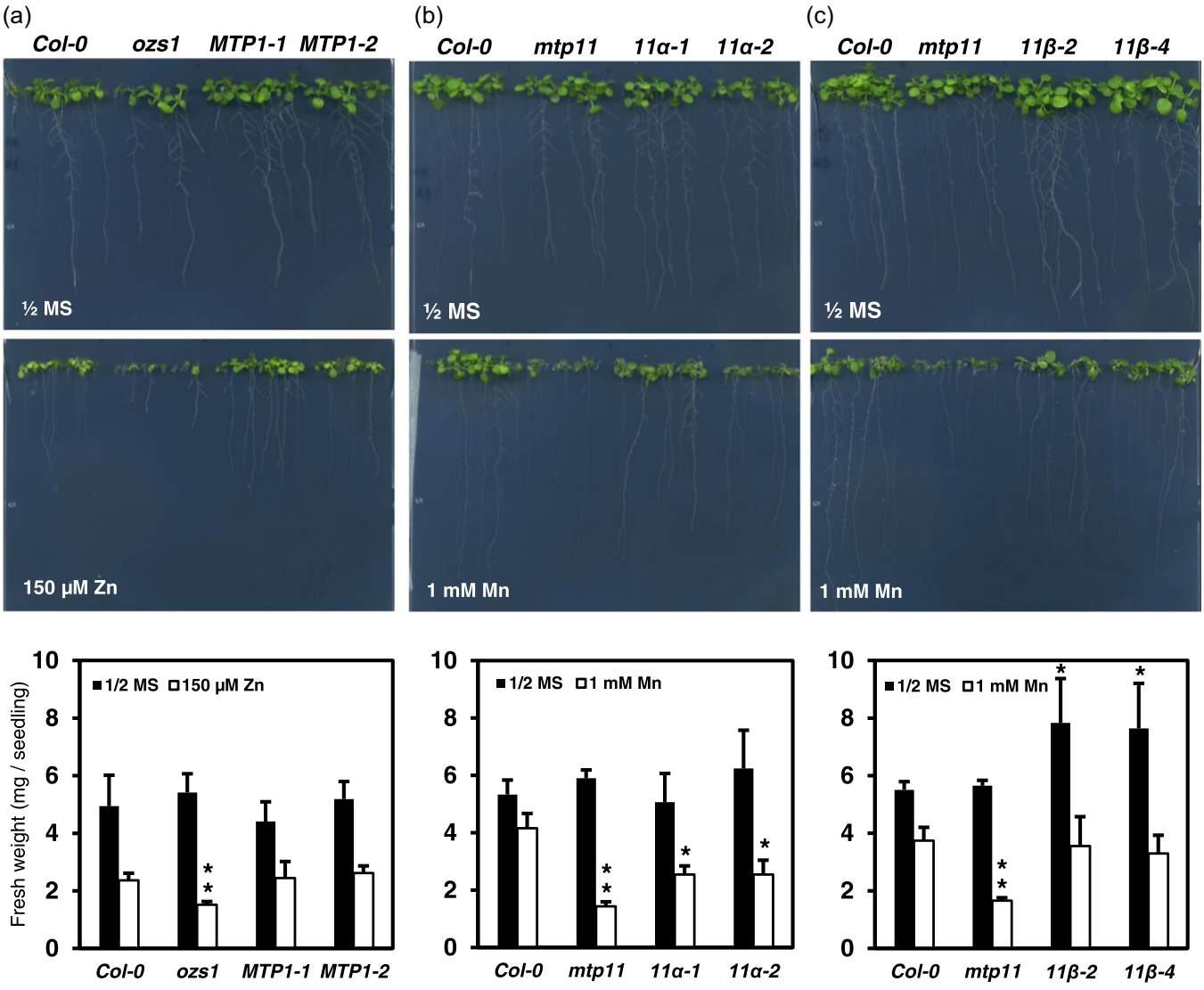

FIGURE 3 Functional complementation of Arabidopsis mutants by *BvMTP*s. The *mtp1* (*ozs1*) and the *mtp11-1* mutant were stably transformed with *BvMTP1* and *BvMTP11α/β*, respectively. Representative images and fresh weights of 14-day-old seedlings grown on media containing 150 µM Zn (a) and 1 mM Mn (b), (c). Two independent lines for each construct are shown. *MTP1-1*, *MTP1-2*: *osz1 35S:BvMTP1*; *11α-1*, *11α-2*: *mtp11-1 35S:BvMTP11α*; *11β-2*, *11β-4*: *mtp11-1 35S:BvMTP11β*. Asterisks indicate statistically significant differences (Student's *t* test; $^{*}p < 0.05$ and $^{**}p < 0.01$).

Arabidopsis *MTP*s. Surprisingly, BvMTP1-mCherry colocalized with AtMTP1-GFP in a vesicular pattern (Figure 4a). However, when both were coexpressed in Arabidopsis protoplasts, they colocalized in the tonoplast, which has been described before as target of AtMTP1 (Desbrosses-Fonrouge et al., 2005). Interestingly, of the closely related BvMTP8.1 and BvMTP8.2, only the former was localized in the tonoplast (Supporting Information: Figure S7). Likewise, a tonoplast localization was found for BvMTP11α, but not for its splice variant BvMTP11β which showed a punctate pattern (Supporting Information: Figure S7). Expression in Arabidopsis protoplasts showed that the localization of BvMTP11ß coincided with that of AtMTP11, which resides in the Golgi (Peiter et al., 2007), while BvMTP11α colocalized with the vacuolar AtMTP1 (Figure 4b). Hence, unlike BvMTP1, localization of BvMTP11 variants was independent of the expression system. The different localizations of the BvMTP8 paralogs and of the BvMTP11 splice variants are suggestive of neofunctionalizations and point to a role of the differential protein parts in their targeting.

As predicted by in silico analyses (Table 1), two family members were found in bioenergetic organelles: BvMTP5 was targeted to chloroplasts, and BvMTP7β to mitochondria, as evidenced by colocalization with a mitochondrial marker (Figure 4b). In addition, BvMTP12 colocalized with a ER marker. Proteins for which a precise localization was not determined are denoted as "endomembrane" in Table 1. These members also have not been localized in Arabidopsis yet.

Taken together, subcellular localization of sugar beet MTPs cannot be directly inferred from their closest Arabidopsis homologs,

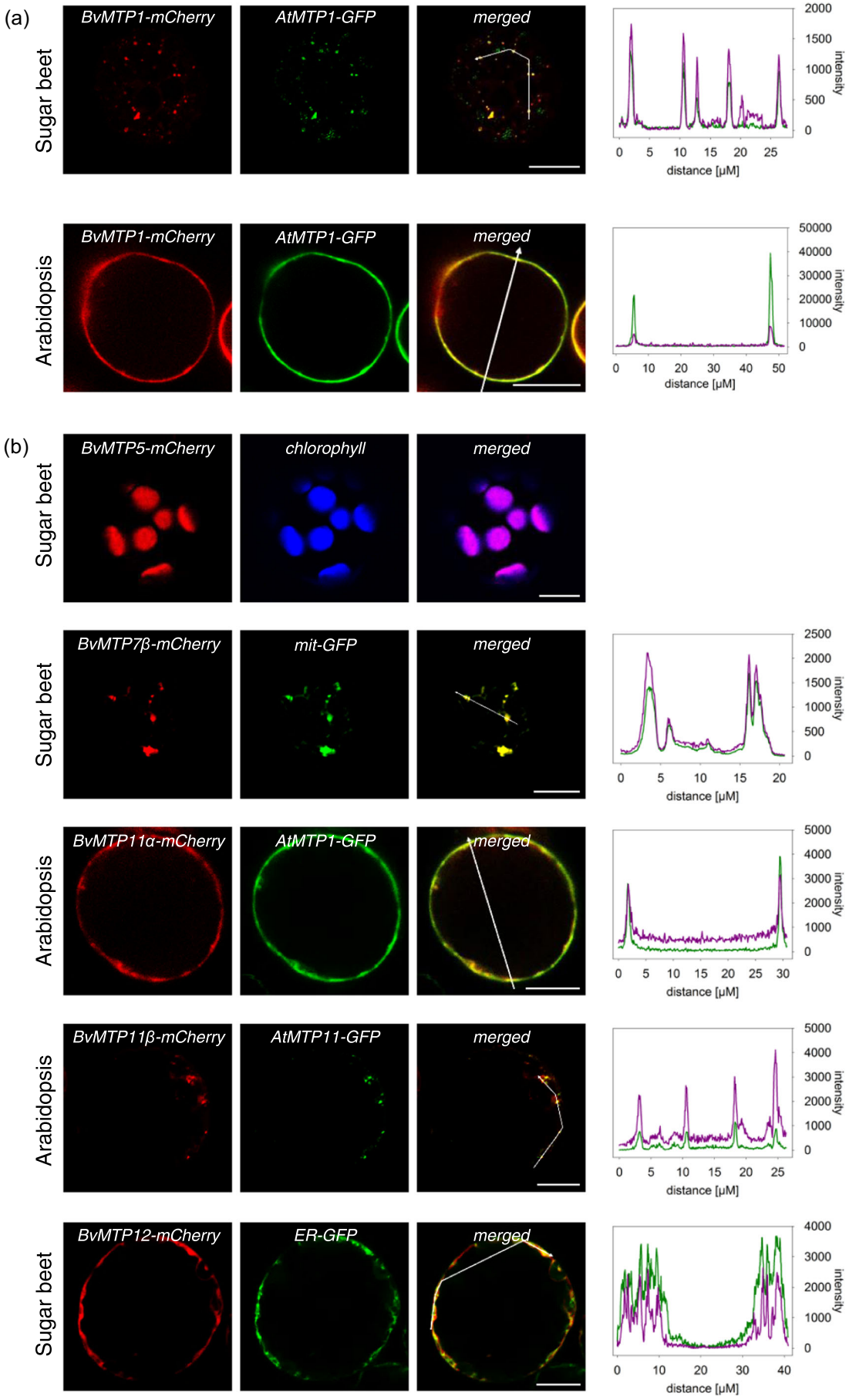

FIGURE 4 (See caption on next page)

and intriguingly, MTP1 transporters showed a punctate pattern or vacuolar localization depending of the plant species in which they were expressed. These results provoke the assumption that the proteins have taken on divergent roles in both plants.

3.6 | *BvMTP* genes have tissue- and age-specific expression patterns

Given the differential substrates and localization of the BvMTP members, we were interested in where and when the genes are expressed. Public RNAseq data of different organs (Dohm et al., 2014) revealed that *BvMTPs* are generally more highly expressed in taproots and seedlings as compared to leaves (Supporting Information: Figure S8a). *BvMTP1* and *BvMTP11α/β* are expressed most homogeneously across tissues, whereas *BvMTP4* shows a low expression, particularly in leaves. Expression in roots and juvenile leaves of 3- to 5-week-old plants, as analysed by qRT-PCR, again differed substantially between family members (Supporting Information: Figure S8b). Interestingly, the splice variants of *BvMTP9* and *BvMTP11* were differentially expressed in leaves and roots. While *BvMTP9β* was detected exclusively in roots, *BvMTP9α* was mainly expressed in leaves at early stages and in roots only at the latest time point analysed in this study. Likewise, *BvMTP11β* was expressed mainly in older roots, whereas *BvMTP11α* was detected in both leaves and roots. In summary, the expression of *BvMTP* genes is dependent on plant tissue and age, what is likely related to differences in micronutrient requirements and homeostasis.

3.7 | Mn-deficient sugar beet accumulates less Fe in roots

In Arabidopsis, MTPs have been associated with the distribution and utilization of micronutrients, and their expression responds to micronutrient availability (Andresen et al., 2018). It is obscure if this extends to other dicot species. In terms of family members, substrates, and localizations, the MTP family in sugar beet has similarities and differences to the phylogenetically distant Arabidopsis. This provoked the question if the responses of MTPs to nutritional imbalances are conserved. However, physiological responses of sugar beet to Mn, Zn, or Fe limitation have not been intensively studied yet, and thus were addressed first.

In other crops, like barley, Mn deficiency often occurs as a latent disorder, without clear visual symptoms in early stages (Schmidt et al., 2013). To investigate the impact of Mn deficiency on sugar beet, seedlings were grown hydroponically on nutrient-replete media and then exposed to Mn-sufficient (+Mn) or Mn-deficient (−Mn) conditions for 12–18 days. The plants displayed typical Mn deficiency symptoms, such as interveinal chlorosis, after 18 days of Mn starvation (Figure 5a,b). Although leaves showed a decrease in chlorophyll content as early as 12 days on −Mn (Figure 5c), no visual chlorotic symptoms were observed at that time. Shoot biomass was not reduced by Mn deficiency in the experimental period, whereas root biomass was decreased relative to +Mn conditions (Figure 5d,e). Thus, sugar beet development was only mildly affected at early stages of Mn deficiency.

To test how Mn deficiency affects the accumulation of macro- and micronutrients in sugar beet, concentrations were analysed in roots and leaves. As expected, the Mn concentration in both plant parts was drastically reduced under low Mn supply (Figure 5f,g). In these plants, Mn concentrations were clearly below the critical threshold described for sugar beet (Draycott, 2006). Unexpectedly, Mn-deficient roots showed a strongly decreased Fe concentration, while no significant differences were observed in leaves. Zn concentrations in leaves and roots remained unaffected by the Mn concentration. In the case of macronutrients, 18 days of Mn deficiency caused a strong depression of K concentrations in roots and leaves (Supporting Information: Figure S9). In roots, but not in leaves, P concentrations were also reduced at both time points, and Mg concentrations at 18 days. The data demonstrate that Mn deficiency causes major alterations in the ionome, particularly a reduction of Fe, K, P, and Mg in roots.

3.8 | Mn deficiency strongly impacts photosynthetic activity in sugar beet leaves

Since Mn is the catalytically active element in the OEC of PSII, minimal fluorescence in the absence of light (F_o), maximal fluorescence (F_m), and maximum quantum yield of PSII photochemistry (F_v/F_m) were analysed by Imaging-PAM fluorometry (Baker, 2008). Interestingly, leaves of plants grown for 12 days in −Mn media showed a decrease in F_v/F_m mainly in the interveinal regions of the proximal part, while the distal area remained largely unchanged compared to +Mn leaves (Figure 6a). Nevertheless, when the whole leaf was averaged, a decrease in F_v/F_m was observed under −Mn, which is mainly due to an increase in F_o, while F_m values remained unchanged (Figure 6b–d). After 18 days of Mn deficiency, F_o was further increased, leading to a further reduction of F_v/F_m. These results demonstrate a close coincidence of loss in chlorophyll and

FIGURE 4 BvMTP proteins are localized to diverse cellular compartments. *BvMTP-mCherry* and *AtMTP1-GFP* expressed in sugar beet and Arabidopsis protoplasts (a). Diverse *BvMTPs* coexpressed with subcellular markers and Arabidopsis *AtMTPs* (b). *mCherry* and *GFP* fusion constructs were transiently expressed in sugar beet or Arabidopsis mesophyll protoplasts for 18 h. The source of the protoplasts is stated on the left. Pixel intensity profiles of GFP (green) and mCherry (magenta) were determined along a virtual line scan. Scale bars represent 10 µm.

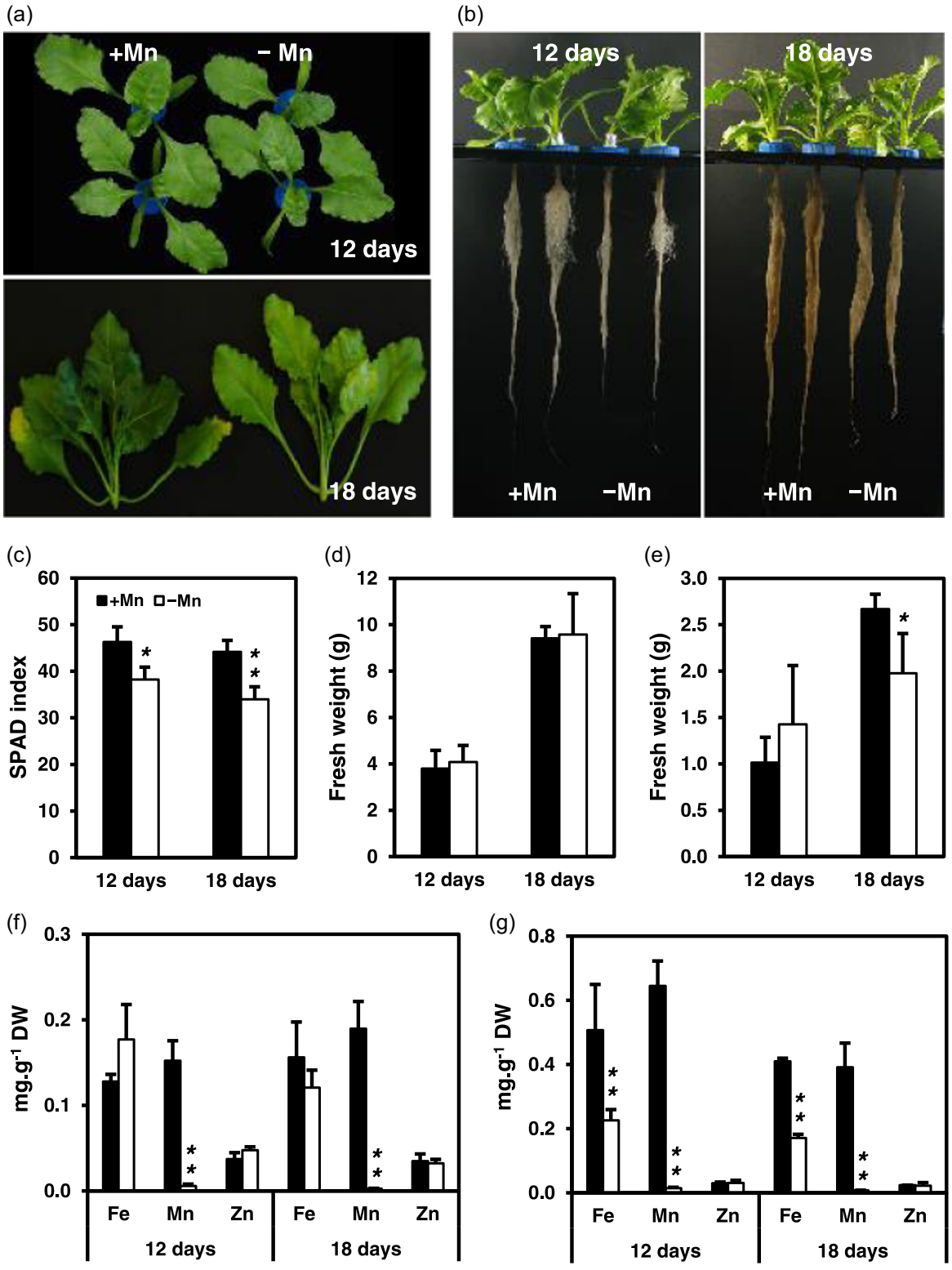

FIGURE 5 Mn deficiency impinges on growth, leaf greenness, and iron accumulation in sugar beet. Shoots (a) and roots (b) of sugar beet plants grown under Mn-replete (+Mn) and Mn-deficient (−Mn) conditions for 12 and 18 days. SPAD index of leaves (c). Fresh weight of leaves (d) and roots (e). Micronutrient concentrations in leaves (f) and roots (g). Values represent the mean ± SD of four biological replicates. Asterisks indicate statistically significant differences of −Mn and +Mn values (Student's *t* test; $^{*}p < 0.05$ and $^{**}p < 0.01$). DW, dry weight.

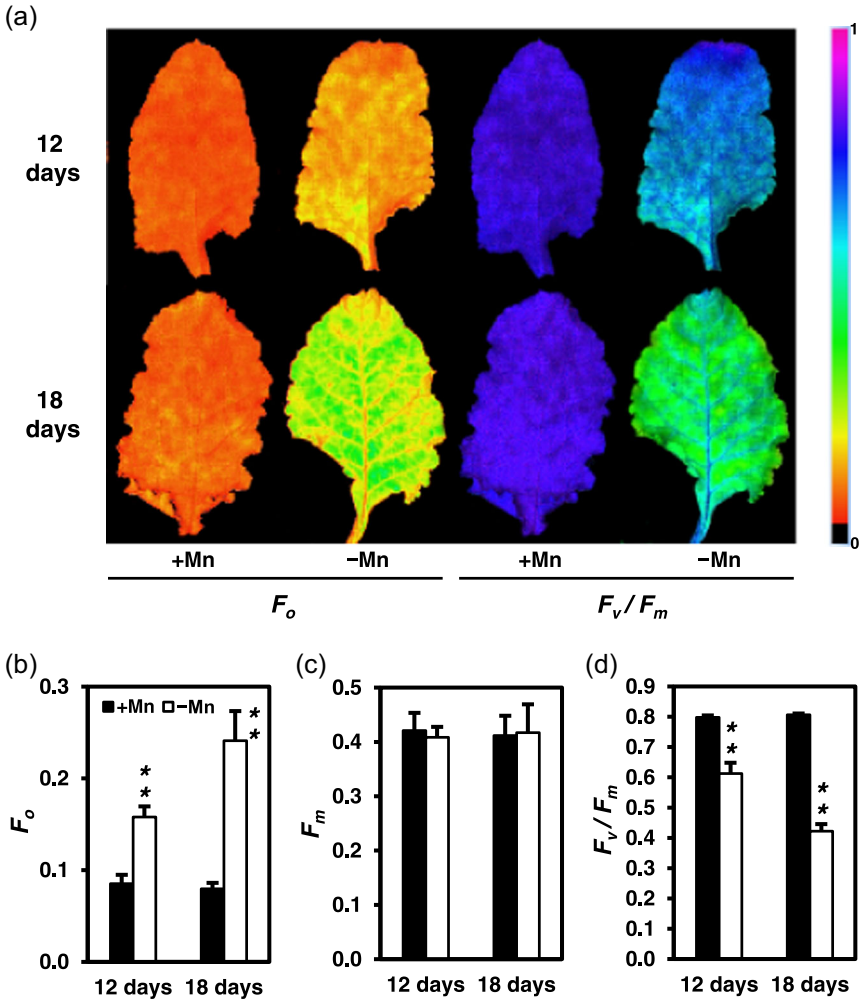

FIGURE 6 Mn-deficient sugar beet plants are defective in PSII activity. Minimum chlorophyll fluorescence (F_0) and maximum PSII efficiency (F_v/F_m) in young leaves grown under Mn sufficiency (+Mn) and Mn deficiency (−Mn) (a). The color scale indicates the relative signal intensities between 0 (black) and 1 (purple). Quantification of F_0 (b), F_m (c), and F_v/F_m (d). Asterisks indicate statistically significant differences of -Mn and +Mn values (Student's *t* test; $^{**}p < 0.01$).

reduction of photosynthetic activity at early stages of Mn deficiency in sugar beet.

3.9 | Mn/Fe-*BvMTP* genes are differentially and splice variant-specifically regulated by low Mn supply

Having established growth conditions to induce Mn deficiency, we determined a possible involvement of *BvMTP*s in the response to those conditions. Transcript levels of the genes were determined in roots and young leaves of plants grown hydroponically under −Mn for 12 days. In young leaves, none of the genes was transcriptionally affected (Figure 7). In contrast, *BvMTP8.2*, which is highly expressed in roots, was upregulated further, whereas its close relative *BvMTP8.1* was downregulated. In *BvMTP11*, only the splice variant *BvMTP11α* was upregulated under Mn starvation. Taken together, transporters of the Mn/Fe subfamily were differentially regulated, which points to their direct involvement in the response to Mn limitation. Intriguingly, the homologs of those transporters in Arabidopsis, AtMTP8 and AtMTP11, are involved in Mn detoxification rather than its efficient utilization.

3.10 | Zn deficiency affects leaf growth without alteration of photosynthetic activity

To analyse the effect of Zn deficiency, sugar beet seedlings germinated on complete media were exposed to Zn-sufficient (+Zn) or Zn-deficient (−Zn) conditions for 12 days. Under Zn deficiency, leaves were smaller, and necrotic areas in leaf margins were observed (Figure 8a). Shoot biomass was significantly reduced, whereas root growth was unaffected (Figure 8b,c). Although leaf growth was reduced in Zn-deficient plants, leaf greenness (SPAD index) and photosynthetic efficiency (F_v/F_m) in nonnecrotic areas was unaffected (Supporting Information: Figure S10a,b), suggesting that the photosynthetic activity in sugar beet plants is not primarily impaired by Zn deficiency.

In Zn-deficient leaves, Zn concentration was reduced to 15% of that in Zn-sufficient plants (Figure 8d); the reduction in roots amounted to 50% (Figure 8e). Interestingly, Zn deficiency caused a significant decrease in Fe and Mn concentrations in leaves and roots, respectively. In addition, macronutrient levels were altered in leaves and roots. While K concentrations were decreased in both parts, Ca concentrations were lower in leaves,

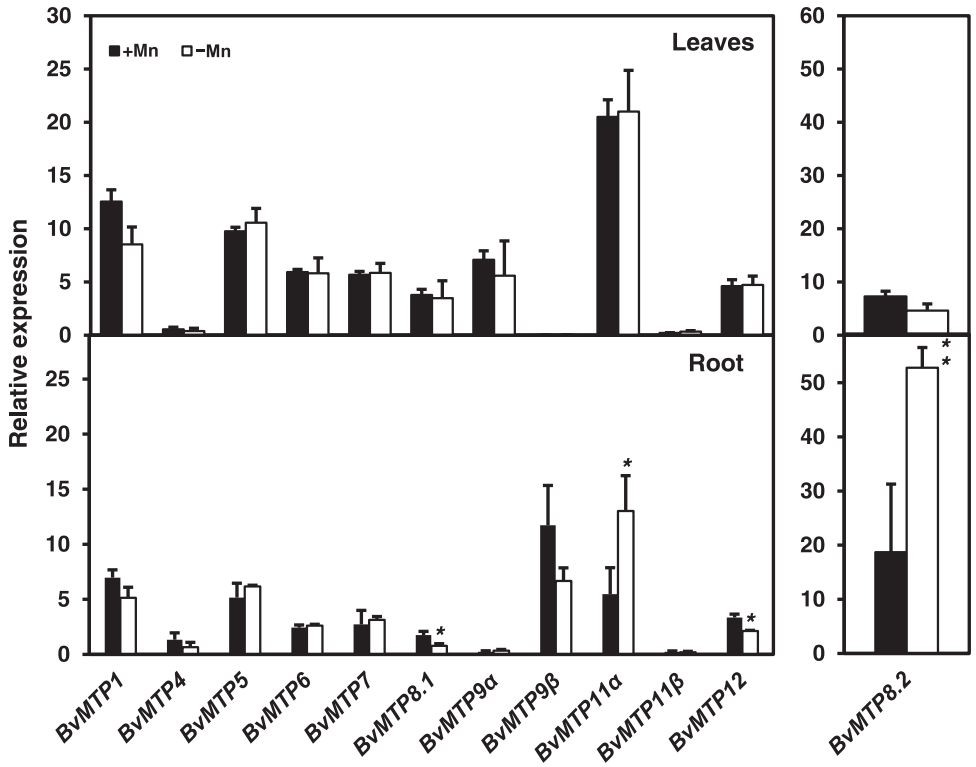

FIGURE 7 Expression of specific *BvMTP* genes is altered by Mn starvation in roots but not in leaves of sugar beet. Plants were cultivated for 12 days under Mn-sufficient (+Mn) or Mn-deficient (−Mn) conditions. Expression of *BvMTP*s was quantified by qRT-PCR. Values represent the mean ± SD of nine qRT-PCR assessments from three independent biological replicates. The average of three housekeeping genes (*BvACT7*, *BvEF1*, *BvGAPDH*) was used as reference value. Asterisks indicate statistically significant differences of −Mn and +Mn values (Student's *t* test; $^*p < 0.05$).

and phosphate concentrations strongly reduced in roots (Supporting Information: Figure S10c,d).

To confirm the Zn-deficient status of the sugar beet plants, a close homolog to the Zn deficiency marker gene *AtIRT3* was identified and named *BvIRT3*. Consistent with the Zn deficiency response in Arabidopsis, *BvIRT3* was upregulated in leaves and roots of sugar beet (Figure 8f).

Notably, none of the *Zn-MTP*s was transcriptionally affected in roots, which deviates from the situation in Arabidopsis, where AtMTP2 is an important component of the Zn deficiency response (Sinclair et al., 2018). The different Zn-responsiveness of Arabidopsis and sugar beet *Zn-MTP*s was confirmed by cultivating Arabidopsis in the same Zn-deficient medium, whereby *AtMTP2* expression in roots showed the previously demonstrated upregulation (Supporting Information: Figure S11).

3.11 | BvMTPs of the Zn subgroup are not induced under Zn deficiency

To investigate whether *BvMTP* genes are transcriptionally regulated by Zn limitation, their expression pattern was determined in roots and leaves of Zn-sufficient and Zn-deficient plants. In leaves *BvMTP1*, *BvMTP7*, and *BvMTP12* were slightly upregulated, whereas *BvMTP6 and BvMTP9α* were downregulated (Figure 9). The only regulated gene in roots was the Mn/Fe-MTP member *BvMTP9α*, but not its splice variant *BvMTP9β* (Figure 9). This gene, which is usually lowly expressed in roots, was highly upregulated there, whereas in leaves its expression was slightly reduced. Given the decrease of Mn concentration in roots under low Zn conditions (Figure 8), the transcriptional regulation of the Mn-transporting BvMTP9α is likely related to Mn homeostasis under low Zn conditions.

3.12 | Plant performance and micronutrient homeostasis of sugar beet are severely affected under Fe deficiency

In Fe-deficient Arabidopsis, low specificity of the Fe uptake transporter IRT1 causes a high accumulation of transition metals which are detoxified by MTP members. To analyse the impact of Fe deficiency on growth and metal accumulation of sugar beet, seedlings grown in complete medium were exposed to Fe-sufficient (+Fe) or Fe-deficient (−Fe) conditions for 5–9 days. Low-Fe plants displayed a strong growth inhibition and leaf chlorosis (Figure 10a–d), reflected in decreased greenness values (Figure 10e). However, unlike in Mn-deficient leaves (Figure 6), F_v/F_m and F_o were not affected in the experimental period (Figure 10f and Supporting Information: Figure S12a,b).

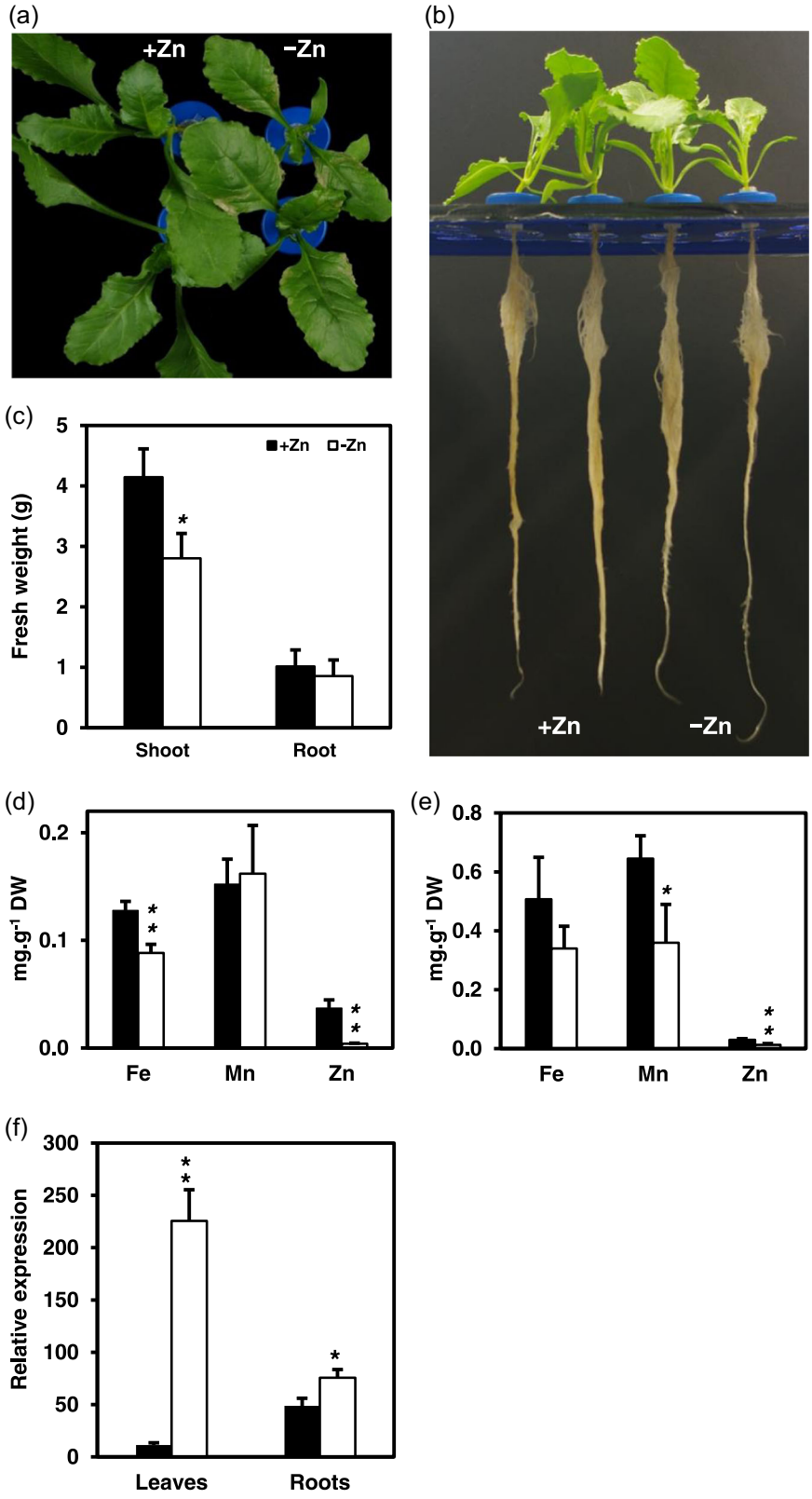

FIGURE 8 Zn deficiency causes necrosis and reduced shoot growth in sugar beet. Shoot (a) and roots (b) of sugar beet plants grown under Zn-sufficient (+Zn) or Zn-deficient (−Zn) conditions. Fresh weight of shoot and roots (c). Concentrations of micronutrients in young leaves (d) and roots (e). Values represent the mean ± SD of four biological replicates. Expression of the Zn deficiency marker gene *BvIRT3* is increased in leaves and roots under Zn starvation (f). Plants were cultivated for 12 days under Zn-sufficient (+Zn) or Zn-deficient (−Zn) conditions. Gene expression was quantified by qRT-PCR. Values represent the mean ± SD of nine qRT-PCR assessments of three biological replicates. The average of three housekeeping genes (*BvACT7*, *BvEF1*, and *BvGAPDH*) was used as reference value. Asterisks indicate statistically significant differences of −Zn and +Zn values (Student's *t* test; $^{*}p < 0.05$ and $^{**}p < 0.01$). DW, dry weight.

Metal accumulation was distinctl altered by Fe deficiency. The Fe concentration decreased strongly in young leaves and even more so in roots under low Fe supply (Figure 10g,h). In parallel, Zn concentration was increased at a low level in roots after 9 days of Fe limitation, while Mn levels were increased already at the first time point and to higher amounts after 9 days. This increase was more pronounced in roots than in leaves, being *c*. fivefold higher in Fe-deficient plants. Concentrations of Ca, K, Mg, and P were not affected by Fe deficiency (Supporting Information: Figure S12c,d).

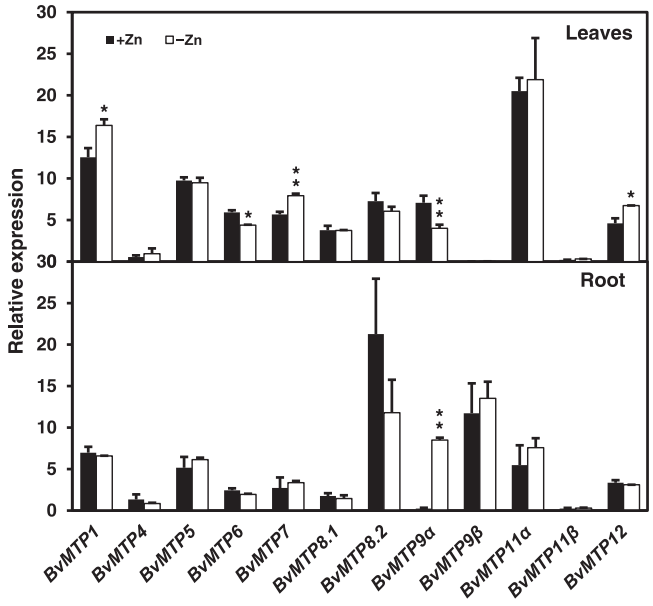

FIGURE 9 Expression of *BvMTP*s is mainly altered in leaves under Zn starvation. Gene expression profile of *BvMTP*s in root and leaves (a). Plants were cultivated for 12 days under Zn-sufficient (+Zn) or Zn-deficient (−Zn) conditions. Gene expression was quantified by qRT-PCR. Values represent the mean ± SD of nine qRT-PCR assessments of three biological replicates. The average of three housekeeping genes (*BvACT7*, *BvEF1*, and *BvGAPDH*) was used as reference value. Asterisks indicate statistically significant differences of −Zn and +Zn values (Student's *t* test; $^{*}p < 0.05$ and $^{**}p < 0.01$).

These results confirm that the chlorotic phenotype was due to primary Fe deficiency and also suggest that sugar beet plants accumulate more Mn when Fe is limiting.

3.13 | Fe deficiency does not induce expression of *BvMTPs* in sugar beet roots

In Arabidopsis, detoxification of the secondary IRT1 substrates is mediated by AtMTP3 and AtMTP8, which handle Zn and Mn, respectively, by sequestration in root vacuoles (Arrivault et al., 2006; Eroglu et al., 2016). It is unknown if this concept extends to dicots in general. Therefore, transcript levels of *BvMTP*s after 9 days of Fe limitation were analysed. Most surprisingly, in roots, the expression of none of the *BvMTP* genes was significantly increased upon Fe starvation (Figure 11a). This also held true for *BvMTP1* and *BvMTP8.1/8.2*, the closest relatives of *AtMTP3* and *AtMTP8*, respectively. In contrast, *BvMTP8.2* was induced *c.* twofold in leaves. To evaluate if the absent upregulation of *BvMTP1* and *BvMTP8.1/8.2* may have been caused by the experimental conditions, Arabidopsis plants were cultivated in the same Fe-deficient medium. The results show that *AtMTP3* and *AtMTP8* expression in roots were induced, as previously described (Supporting Information: Figure S13). These results suggest that positive transcriptional responses of *MTPs* to Fe deficiency in sugar beet occur exclusively in leaves, albeit not very pronounced, which is in stark contrast to Arabidopsis.

3.14 | Fe deficiency-responsive genes are differentially regulated in leaves and roots of sugar beet

The unresponsiveness of *Mn/Fe-* and *Zn-MTP* members to Fe deficiency provoked the question if other parts of the Fe deficiency response are conserved. In Arabidopsis, the expression of the ZIP transporter genes *IRT1* and *IRT2* is under control of the transcription factor FIT, which itself is transcriptionally upregulated, whereas the Fe storage protein FERRITIN1 (FER1) is downregulated by Fe deficiency (Schwarz & Bauer, 2020). To gain an insight into the sugar beet response to Fe deficiency, *IRT*, *FIT*, and *FER1* homologs were identified and their expression analysed. Consistent with the Fe deficiency response in Arabidopsis, *BvFIT* and *BvFER1* were upregulated in roots and downregulated in leaves, respectively (Figure 11b,c). In addition to *IRT3*, another two *BvIRT* genes were identified in the sugar beet genome and named *BvIRT1* and *BvIRT2*, according to their similarity to Arabidopsis *IRT*s. In roots, *BvIRT1* was upregulated, while *BvIRT3* expression was unaffected under Fe deficiency (Figure 11c). Conversely, *BvIRT3* was upregulated, albeit on a low absolute expression level, in young leaves (Figure 11b). *BvIRT2* was expressed neither in root nor young leaves regardless of the Fe treatment. These results strongly suggest that BvIRT1 is the main Fe uptake transporter under Fe deficiency. Key players of the Fe deficiency response known from Arabidopsis are thus also induced in sugar beet, albeit differences are apparent, such as absent expression of *BvIRT2*.

3.15 | Mn and Zn excess promote Fe accumulation in sugar beet, and Zn surplus induces expression of *BvMTPs*

In Arabidopsis, Mn and Zn excess provoke Fe deficiency and induce *MTP* genes. While Mn excess causes a FIT-dependent upregulation of *AtMTP8* expression (Eroglu et al., 2016), Zn toxicity induces *AtMTP3* (Arrivault et al., 2006; Shanmugam et al., 2011). Since *MTP*s were largely unresponsive to primary Fe deficiency in sugar beet (Figure 11a), we asked if its response to either Mn or Zn excess also differs from that in Arabidopsis. To this end, plants were grown for three days with high Mn (500 µM $MnSO_4$), high Zn (200 µM $ZnSO_4$), and standard supply (5 µM $MnSO_4$, 0.3 µM $ZnSO_4$). In high-Mn media, Mn was increased *c.* 10-fold in leaves and *c.* threefold in roots (Figure 12a,b). Even more severely, Zn concentration was increased up to 20-fold in leaves and 70-fold in roots of plants grown under high Zn. In leaves, Mn and Zn excess led to a decrease in Fe and Mn, respectively (Figure 12a). Unexpectedly, the Fe concentration in roots was increased under both high Mn and Zn, which is in contrast to Arabidopsis and other species, where it is unaffected or

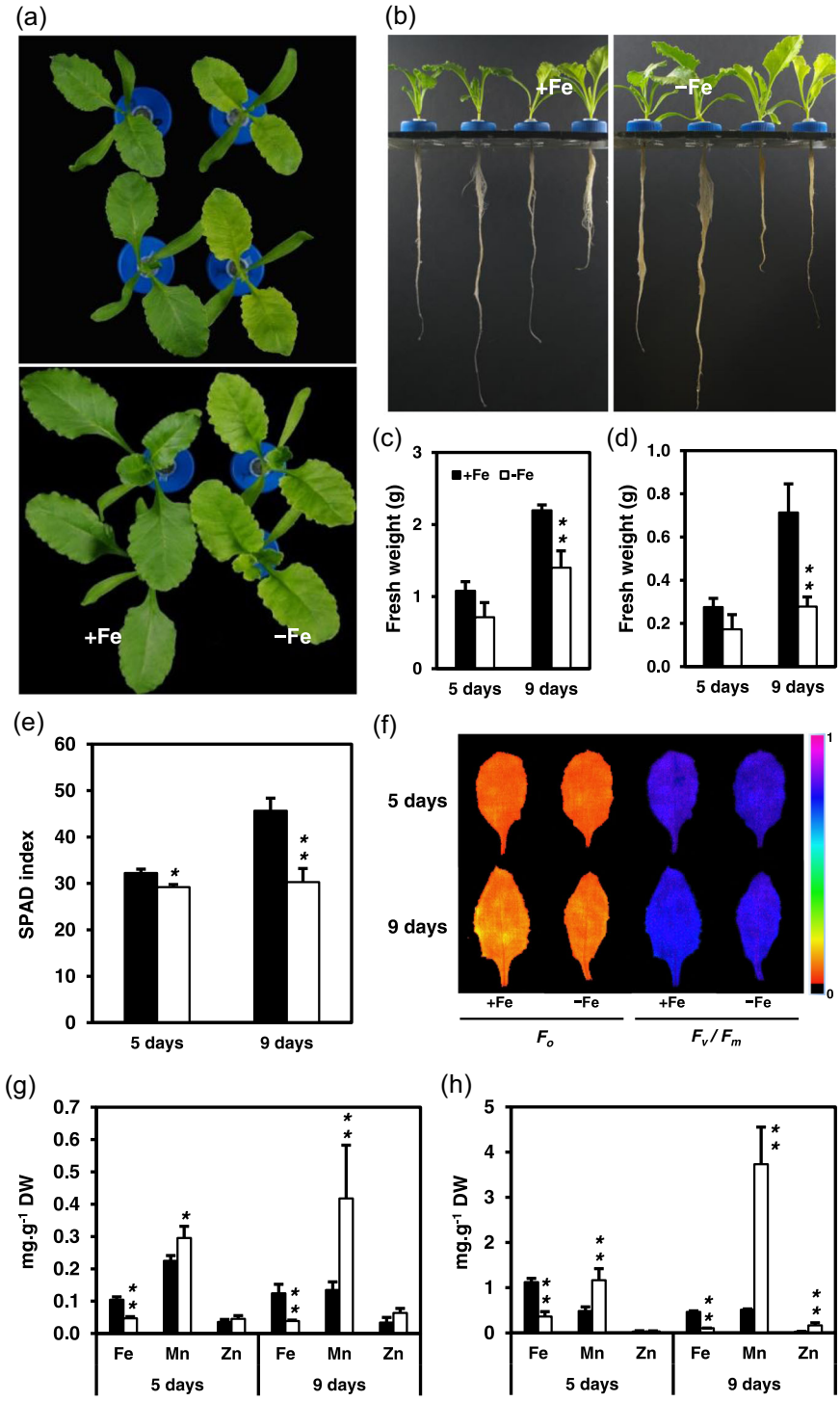

FIGURE 10 Sugar beet plants show growth defects in leaves under low Fe conditions. Shoot (a) and roots (b) of sugar beet plants grown under Fe-sufficient (+Fe) or Fe-deficient (−Fe) conditions. Fresh weight of shoot (c) and roots (d). SPAD index of leaves (e). Minimum chlorophyll fluorescence (F_0) and maximum photosystem II (PSII) efficiency (F_v/F_m) in young leaves (f). The color scale indicates relative signal intensities from 0 (black) to 1 (purple). Concentrations of micronutrients in young leaves (g) and roots (h). Values represent the mean ± SD of four biological replicates. Asterisks indicate statistically significant differences of −Fe and +Fe values (Student's *t* test; $^*p < 0.05$ and $^{**}p < 0.01$). DW, dry weight.

reduced by Mn and Zn toxicity (Eroglu et al., 2016; Lešková et al., 2017). Concentrations of the macronutrients K, Ca, Mg, and P remained unchanged under Mn excess (Supporting Information: Figure S14a,b), while the K concentration was reduced in roots and the concentrations of Ca, K, and Mg were reduced in leaves of high-Zn plants.

In Arabidopsis, excess Mn is detoxified by AtMTP8, which is transcriptionally upregulated (Eroglu et al., 2016). Again, this was not found in sugar beet, where none of the *BvMTPs* responded notably (Figure 12c). By contrast, very strong upregulation of *Zn-MTP* transporters, in particular *BvMTP1* and *BvMTP4*, was observed under Zn excess in leaves and roots. Intriguingly, the Mn transporter *BvMTP9α*, that was induced in roots by Zn deficiency (Figure 9), was also strongly upregulated by Zn excess (Figure 12c).

As Mn and Zn excess caused an unexpected rise in root Fe accumulation (Figure 12a), we determined the expression of genes involved in the plant's Fe deficiency response. In leaves, *BvFER1* expression was downregulated and *BvIRT3* unaffected

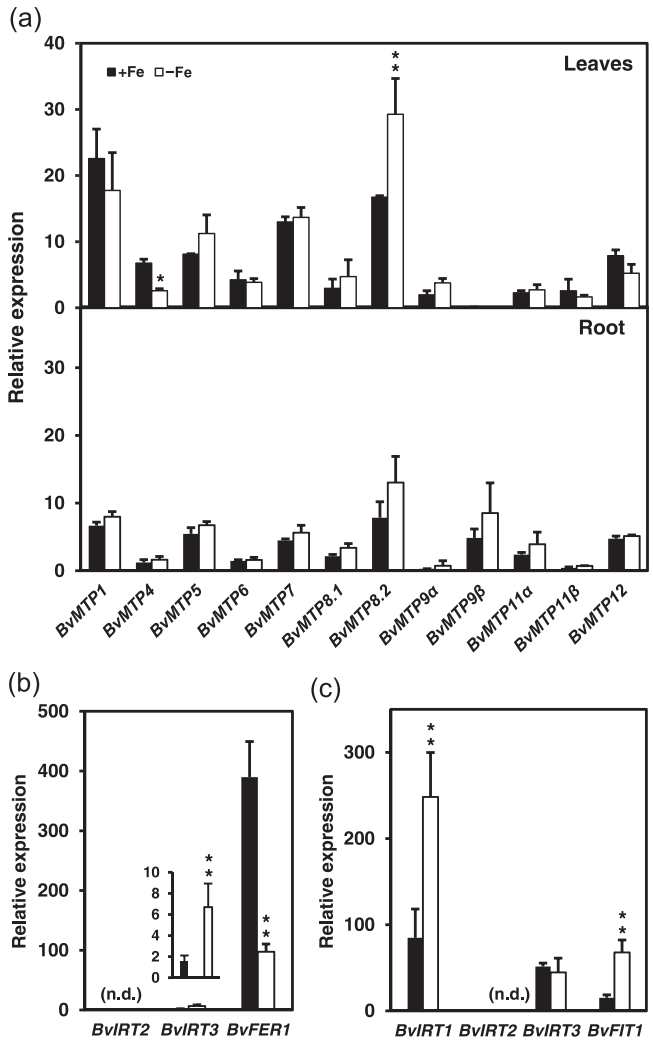

FIGURE 11 Expression of specific *BvMTP*s and Fe deficiency marker genes is altered by Fe starvation. Plants were cultivated for 9 days under Fe-sufficient (+Fe) or Fe-deficient (−Fe) conditions. Expression of *BvMTP*s (a). Expression of Fe deficiency marker genes in leaves (b) and roots (c). Gene expression was quantified by qRT-PCR. Values represent the mean ± SD of nine qRT-PCR assessments of three biological replicates. The average of three housekeeping genes (*BvACT7*, *BvEF1*, and *BvGAPDH*) was used as reference value. Asterisks indicate statistically significant differences of −Fe and +Fe values (Student's *t* test; $*p < 0.05$ and $**p < 0.01$).

under both conditions (Supporting Information: Figure S14c), while in roots, *BvIRT1*, *BvIRT3*, and *BvFIT1* were upregulated (Supporting Information: Figure S14d), causing, very likely, the increased Fe level in roots.

3.16 | *BvIRT*s complement yeast mutants defective in Fe, Mn, and Zn uptake

MTP-based detoxification mechanisms for Mn and Zn were not activated in sugar beet subjected to Fe limitation or Mn excess, albeit *BvIRT1* was induced. Also, Fe accumulation was increased in high-Mn and high-Zn plants, coinciding with an upregulation of *BvIRT1*. Since in Arabidopsis, this transporter imports large amounts of Mn and Zn, besides Fe, we hypothesized that sugar beet IRT1 may be more Fe-selective. To determine the substrate specificity of the IRT transporters, yeast complementation assays were performed. Expression of the splice variants *BvIRT1α* and *β*, as well as *BvIRT3α* and *β* restored the ability of the Fe uptake-defective mutant Δ*fet3*Δ*fet4* to grow on a medium supplemented with the Fe chelator BPDS (Supporting Information: Figure S15a). However, *BvIRT1α* and *β* only partially complemented the Δ*fet3*Δ*fet4* phenotype, as compared to *AtIRT1*, whereas *BvIRT3α* and *β* were more efficient.

To assess Mn transport, the *BvIRT*s were expressed in the Mn uptake-defective mutant Δ*smf1*, which is unable to grow under low Mn supply. Interestingly, only *BvIRT1α* and *β* were able to rescue the growth of Δ*smf1* as efficiently as the Mn uptake transporter *AtNRAMP1* on medium containing the Mn chelator EGTA (Supporting Information: Figure S15a). Moreover, *BvIRT1*s and *BvIRT3*s fully complemented the Zn uptake-defective mutant Δ*zrt1*Δ*zrt2*, which is unable to grow under low Zn supply (Supporting Information: Figure S15b). *BvIRT2* partially complemented the Δ*zrt1*Δ*zrt2* mutant, but was not able to complement the Fe or Mn uptake-defective yeast mutants. These results indicate that BvIRT1*α* and *β* may mediate Fe, Mn, and Zn transport, whereas BvIRT3*α* and *β* may only transport Fe and Zn, alike their Arabidopsis counterparts (Lin et al., 2009; Vert et al., 2002). The observed differences in Fe accumulation between Arabidopsis and sugar beet cannot be explained by different substrate spectra of their IRT1 proteins.

4 | DISCUSSION

Essential metal imbalances affect plant performance. They may decrease photosynthetic activity and other processes, which in turn leads to a reduced plant growth. Short-term deficiencies of Fe and Zn, but not Mn affected leaf biomass accumulation of sugar beet, while only the latter reduced PS II efficiency and in particular root growth to a large extent. Elemental concentrations were also altered, sometimes in unexpected ways. However, mechanisms of transition metal homeostasis are largely obscure in this non-model plant. Numerous studies have led to models in which MTP proteins are central to metal handling in plants, which is also reflected in their transcriptional regulation. Although MTP proteins have been described in diverse plant species, those concepts are primarily derived from work on Arabidopsis and rice. This focus on a very limited number of model species provokes the question to what extent our mechanistic understanding derived from those studies can be extrapolated to other plants, in particular economically important crops. We addressed this issue for sugar beet, which, belonging to the Caryophyllales, is phylogenetically distant from Arabidopsis. Following the identification of all *BvMTP* members and splice variants, the analysis of subcellular localization, substrate spectrum, and transcriptional regulation upon defined nutritional imbalances revealed unexpected deviations from their Arabidopsis counterparts.

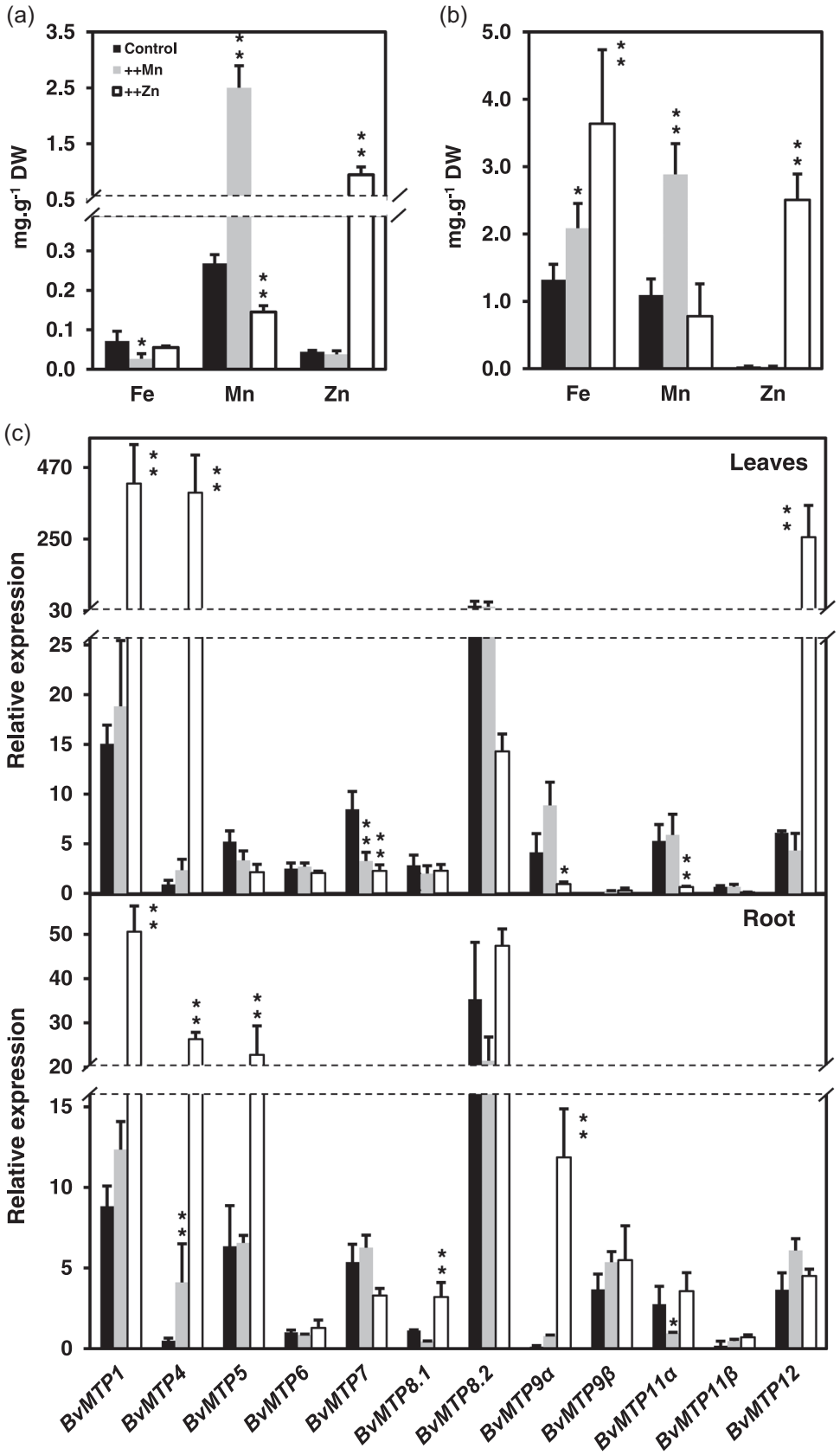

FIGURE 12 Elemental concentrations and expression of *BvMTPs* are affected under Mn and Zn excess. Sugar beet plants were treated for 5 days with 500 µM $MnSO_4$ (++Mn) or 200 µM $ZnSO_4$ (++Zn). Concentrations of micronutrients in young leaves (a) and roots (b). Expression of *BvMTPs* quantified by qRT-PCR (c). Values represent the mean ± SD of nine qRT-PCR assessments of three biological replicates. The average of three housekeeping genes (*BvACT7*, *BvEF1*, and *BvGAPDH*) was used as reference value. Asterisks indicate statistically significant differences (Student's *t* test; $^{*}p < 0.05$ and $^{**}p < 0.01$).

4.1 | A functional characterization of sugar beet MTP transporters

A phylogenetic analysis showed that all BvMTP proteins of sugar beet have a homolog in Arabidopsis (but not vice versa) and that these proteins can be classified into three subgroups: Zn-MTPs, Fe/Zn-MTPs, and Mn/Fe-MTPs (Figure 1). BvMTP1 and BvMTP4 contain the conserved motifs in TMD-II and TMD-V, as well as the H/S region present in other Zn-MTPs (Montanini et al., 2007). As expected for a member of the Zn-MTP cluster, BvMTP1 complemented the Zn hypersensitivity phenotype of the Δ*zrc1* yeast mutant (Figure 2). BvMTP1 is most closely related to AtMTP1, 3, and 2 of Arabidopsis, of which the former two are localized in the tonoplast (Arrivault et al., 2006; Desbrosses-Fonrouge et al., 2005), and the latter one in the ER (Sinclair et al., 2018). Interestingly, BvMTP1 is localized in a non-vacuolar endomembrane compartment when expressed in sugar beet protoplasts, but it was targeted to the tonoplast when expressed heterologously in Arabidopsis protoplasts (Figure 4a). Intriguingly, AtMTP1 also displayed these divergent localization patterns in both species. This might indicate that MTP1 transporters recycle from tonoplast to nonvacular endomembranes, possibly determined by internal Zn status, and that protoplasts of both species reflected a different physiological state. Alternatively, MTP1 may continuously reside in a vesicular compartment in sugar beet. The Zn-MTP member BvMTP4, which also localized to an endomembrane compartment, did not complement any of the tested yeast mutants. In contrast, its Arabidopsis homolog AtMTP4 allowed a Δ*zrc1*Δ*cot1* strain to grow on Zn-supplemented medium and rescued a growth defect of a yeast lacking MSC2, the ortholog of AtMTP12 (Fujiwara et al., 2015). Therefore, BvMTP4 is likely involved in Zn supply of a metabolically active compartment. A role of BvMTP4 in Zn detoxification may be indicated by its strong upregulation under high Zn load (Figure 12).

Similar to AtMTP12, the Zn-MTP protein BvMTP12 has unique structural characteristics, such as twice the length compared to the other BvMTPs and a long cytosolic loop between TMDs IV and V. Interestingly, while BvMTP12 presents all specific domains of Zn-MTP proteins, its closest relative BvMTP5 harbors a change from D to G in the HxxxD motif in TMD II and has no cytosolic loop. These particular characteristics are also present in MTP5 and MTP12 homologs of other species (Fujiwara et al., 2015; Ram et al., 2019). In Arabidopsis, both proteins are believed to form a heteromeric complex with Zn transport activity in the Golgi (Fujiwara et al., 2015). Owing to the lack of Zn-MTP domains, MTP5 may serve as regulatory subunit for MTP12 rather than operating as Zn transporter. Surprisingly, in sugar beet, BvMTP5 is localized in chloroplasts, while BvMTP12 is located in the ER, pointing to a function in its own right (Figure 4b). In plants, no MTP has been localized to the chloroplast so far. Further investigations are necessary to understand the physiological role of BvMTP5 in chloroplasts, in particular as its presumed interaction partner is localized in a different compartment.

The plant Fe/Zn-MTP cluster can be divided into two groups, containing MTP6 and MTP7 proteins (Ricachenevsky et al., 2013). Interestingly, AtMTP6 and AtMTP7 contain a putative mitochondrial transit peptide, but experimental evidence of their subcellular localization and substrates are missing. In the present study, sugar beet BvMTP7β was indeed localized to mitochondria (Figure 4), consistent with the presence of a mitochondrial targeting sequence. By contrast, BvMTP6 was located in endomembranes. Similar to their Arabidopsis homologs (Fujiwara et al., 2015), these proteins did not restore the growth of any metal-sensitive yeast mutant, asking for further analyses to determine their substrates and physiological roles.

Mn/Fe-MTPs are well-known to mediate Mn transport in different plant species, and AtMTP8 has also been described to transport Fe (Alejandro et al., 2020; Eroglu et al., 2017). In sugar beet, all proteins belonging to the Mn/Fe-MTP cluster contain the conserved motif DxxxD, and all Mn/Fe-BvMTPs alleviated the Mn hypersensitivity of a Δ*pmr1* yeast mutant (Figure 2). Sugar beet owns two AtMTP8 homologs, BvMTP8.1 and 8.2, that are both able to transport Mn and Fe when are expressed in yeast cells. However, these proteins are located in different subcellular compartments (Figure 4). While BvMTP8.1 is localized in the tonoplast, BvMTP8.2 shows a punctate localization pattern. Localization of MTP8 proteins has been observed before to differ between species: tonoplast-localized MTP8 homologs in Arabidopsis, rice, and white lupin are implicated in vacuolar Mn sequestration (Chen et al., 2013; Eroglu et al., 2016; Olt et al., 2022; Takemoto et al., 2017), while in barley, HvMTP8.1 and HvMTP8.2 are located in the Golgi with unknown function (Pedas et al., 2014). So far sugar beet is the only plant with two differently localized MTP8 proteins, indicating a diversification in their roles. However, it cannot be excluded that their subcellular localization is regulated by metal concentrations, as previously shown for IRT1 and NRAMP1 in Arabidopsis (Agorio et al., 2017; Barberon & Geldner, 2014).

Alternative splicing, by which multiple messenger RNA variants are produced from a single gene, increases protein diversity and is an additional regulatory point of gene function. It occurs mainly in response to environmental stresses such as heat, cold, salt, drought, and nutrient deficiency (Filichkin et al., 2015). Indeed, recent studies have shown that nutrient-specific regulation of splicing contributes to the homeostasis of nutrients in rice, including Fe, Mn, and Zn (Dong et al., 2018). MTP splice variants have been annotated in Arabidopsis (http://aramemnon.uni-koeln.de/index) and rice (http://rice.plantbiology.msu.edu/), suggesting that selective splicing of MTP proteins may be a common regulatory mechanism in plants. In sugar beet, two Mn/Fe-MTPs, *BvMTP9* and *11*, show a pair of splice variants resulting from alternative start codons. As the first exon encodes a putative cytosolic N-terminus, BvMTP9α and β, as well as BvMTP11α and β, share TMDs and conserved domains. The BvMTP9 variants resulted in a similar punctate localization pattern. Both were able to transport Mn in Δ*pmr1* yeast, but, intriguingly, only *BvMTP9β* complemented the Fe-sensitive phenotype of Δ*ccc1*. An effect of splicing on transport competence has previously been shown for AtNRAMP6 (Cailliatte et al., 2009); however, the determination of substrate selectivity by alternative splicing has not been described yet, and may present another layer of regulation yet to be addressed.

In Arabidopsis and rice, MTP9/10 homologs have been described to only transport Mn, but not Fe (Chu et al., 2017; Ueno et al., 2015). By contrast, PbMTP9 and 10 of pear transport both Mn and Fe (Hou et al., 2019). It has been proposed that the presence of a conserved D/ExxD/E motif is crucial for the ability of Mn/Fe-MTPs to transport Fe (Chu et al., 2017). This motif is present in AtMTP8, but not in AtMTP9, 10, and 11. Interestingly, the motif is also found in the N-terminus of BvMTP9β, but not α, which supports its function as determinant of Fe transport.

Both splice variants of BvMTP11 complemented the Mn-sensitive phenotype of the Δ*pmr1* mutant (Figure 2), but while BvMTP11β showed a punctate pattern which colocalized with AtMTP11, BvMTP11α is located in the tonoplast (Figure 3b and Supporting Information: Figure S8). This finding is again intriguing, as it suggests that targeting may be governed by alternative splicing, another layer of regulation yet to be addressed. In Arabidopsis, a dileucine motif [(D/E)X_{3-5}L(L/I)] in the N-terminus has been identified to sort plant membrane proteins to the tonoplast (Komarova et al., 2012; Müdsam et al., 2018). The presence of this motif in BvMTP11α but not β (Supporting Information: Figure S2b) is the likely factor for its targeting to the tonoplast, which needs to be experimentally confirmed. Since no other MTP11 homolog has been found in the vacuole yet (Delhaize et al., 2007; Farthing et al., 2017; Ma et al., 2018; Peiter et al., 2007), BvMTP11α may perform a role in sugar beet that is not taken on by MTP11s in other species. However, as both splice variants complement the Mn sensitivity of the Arabidopsis *mtp11-1* mutant (Figure 3), it can be assumed that the both remove Mn from the cytosol under toxic concentrations.

4.2 | The impact of micronutrient deficiencies on sugar beet

Mn-deficient sugar beet leaves showed interveinal chlorosis and a decrease in chlorophyll content (Figure 5), which is a typical symptom for this disorder. It has been proposed that the reduced activity of the OEC by low Mn availability causes the disintegration of PSII complexes which directly affects thylakoid structure and promotes chlorophyll degradation leading to the development of chlorotic leaves (Alejandro et al., 2020). Similarly, Fe deficiency induces interveinal chlorosis owing to its essential role in chlorophyll biosynthesis (Briat et al., 2015). As expected, sugar beet plants with low Fe supply were smaller and contained less chlorophyll compared to Fe-sufficient plants (Figure 10). Visual Fe deficiency symptoms in leaves were observed after as early as five days, while symptoms of Mn deficiency appeared only after a prolonged treatment of 18 days. At an earlier time point, changes in photosynthetic parameters were apparent despite the absence of visually discernible symptoms, what has been called "latent Mn deficiency" in barley (Hebbern et al., 2009). The appearance of Mn deficiency in sugar beet is thus highly influenced by the length and strength of the limitation. Since root Mn pools may be remobilized to supply the shoot (Maillard et al., 2015; Pottier et al., 2019), the length of the growth period in Mn-replete medium before Mn shortage is likely to determine the onset of Mn deficiency symptoms. Further experiments are required to determine the importance of the root Mn pool in sugar beet, and indeed any species, for Mn remobilization under Mn limitation. Also, the mechanisms that mediate this remobilization are not clear yet.

Unlike early Fe deficiency, Mn deficiency causes a specific inactivation of the photochemical reaction in PS II, which leads to a strong reduction of the electron flow (Schmidt et al., 2016). Hence, a decrease in the F_v/F_m value (whereby $F_v = F_m - F_o$) is a useful parameter to detect Mn deficiency in plants before visual deficiency symptoms, what has found practical applications in barley (Schmidt et al., 2013). Barley plants grown under Mn-limited conditions showed lower F_m values, while F_o remains largely unaffected (Schmidt et al., 2013). Interestingly, although sugar beet leaves showed similarly decreased F_v/F_m values under Mn deficiency (Figure 6), this was due to an increase in F_o instead of a decrease in F_m. Further work is required to understand the mechanistic basis of the different Mn-inflicted changes in the chlorophyll fluorescence parameters in different plant species.

Low Zn supply generally causes the inhibition of protein synthesis and leads to increased ROS levels resulting from lower Cu/Zn-SOD activity (Cakmak, 2000). Zn deficiency also reduces chlorophyll content and inhibits PSII activity. Consequently, typical deficiency symptoms include leaf chlorosis, necrotic spots, photosynthesis inhibition, and impaired growth (Alloway, 2009). In this study, sugar beet plants also showed necrotic areas in leaves and a decrease in biomass under Zn deficiency (Figure 8). However, although Zn concentrations in leaves were below the critical threshold (Draycott, 2006), chlorophyll content and photosynthetic activity were not affected by Zn deficiency. It would thus be interesting to determine whether mechanisms to maintain photosynthesis under Zn starvation are superior in sugar beet as compared to other plants, likely either by improving subcellular Zn allocation or better Mn and Fe homeostasis in chloroplasts.

4.3 | Micronutrient homeostasis in sugar beet and the involvement of BvMTPs

The nutritional imbalances imposed in the present study triggered specific changes in the ionome and transcriptional responses of *BvMTP*s, with a number of notable differences to responses of Arabidopsis. While not affecting Fe concentrations in shoots, Mn deficiency may cause increased Fe levels in roots of Arabidopsis (Cailliatte et al., 2010), which, however, is not always observed (Lanquar et al., 2010). In sugar beet leaves, Fe concentrations remained similarly unaffected by Mn deficiency, but roots showed an unexpected decrease in Fe (Figure 4). Such a decreased accumulation of Fe under Mn deficiency has not been described before, and requires further investigations. It may be hypothesized that under Mn deficiency, Fe is remobilized from root vacuoles alongside Mn by poorly selective NRAMP transporters (Lanquar et al., 2010), in parallel with a reduced Fe uptake. A decreased Mn and Fe

sequestration in Mn-deficient roots, hence increasing Mn translocation to the shoot, is supported by the downregulation of the vacuolar Mn/Fe-MTP *BvMTP8.1* (Figure 7). This parallels the downregulation of its Arabidopsis homolog, AtMTP8, upon Mn deficiency (Yang et al., 2008). A similar mechanism has been proposed to operate under Fe deficiency in Arabidopsis, whereby the expression of vacuolar Fe transporters (AtVTLs) is decreased (Gollhofer et al., 2014). However, another tonoplast-localized Mn/Fe-MTP, *BvMTP11α*, was upregulated in Mn-deficient roots (Figure 7), what apparently contradicts this hypothesis and asks for an expression analysis with higher spatiotemporal resolution. The selectivity of BvMTP11α against Fe (Figure 2) may explain the decreased Fe accumulation in Mn-deficient roots. The strongly expressed *BvMTP8.2*, encoding a Mn/Fe transporter in endomembranes (Supporting Information: Figure S7), is also upregulated under Mn deficiency (Figure 7). This renders it highly unlikely that it has a comparable function as its Arabidopsis counterpart, AtMTP8. Instead, BvMTP8.2 may contribute to Mn efficiency by mediating its transfer towards the shoot, similar to OsMTP9 in rice (Ueno et al., 2015).

Arabidopsis responds to Zn deficiency with a systemically controlled upregulation of *AtHMA2*, encoding a heavy metal ATPase to load the xylem, and *AtMTP2*, which encodes an ER-localized transporter of the Zn-MTP subgroup (Sinclair et al., 2018). The response of *AtMTP2* to Zn deficiency was confirmed in this work (Supporting Information: Figure S11). AtMTP2 is proposed to facilitate movement of Zn within the root ER, which may improve Zn translocation. Several pieces of evidence point to an absence of the latter mechanism in sugar beet. First, only one homolog of AtMTP1, 2, and 3 is present in the genome (Figure 1); second, this protein, BvMTP1, is not localized in the ER (Figure 4); third, *BvMTP1* is not upregulated under Zn deficiency in roots. This puts the general importance of intra-ER Zn translocation into question, what is of particular importance in the endeavor to improve Zn accumulation in edible parts of crops (Sinclair et al., 2018). It remains to be studied how widespread a Zn translocation mechanism based on MTP2 is amongst plant and crop species.

In Arabidopsis, Fe deficiency provokes major disruptions in the ionome. It entails an accumulation of Zn in shoots, and even more so in roots (Eroglu et al., 2016; Lešková et al., 2017; Vert et al., 2002), caused by the induction of the poorly specific Fe uptake transporter AtIRT1. The inevitably accumulated Zn is detoxified by vacuolar sequestration mediated by AtMTP3, a Zn-MTP whose expression is strongly upregulated under Fe deficiency (Arrivault et al., 2006; Yang et al., 2010), as also found in this study (Supporting Information: Figure S13). As expected, the sugar beet IRT1 homolog was also transcriptionally upregulated in plants that suffered Fe deficiency, as evident from chlorosis and growth depression (Figures 10 and 11). However, Zn concentrations in leaves were not increased, and those in roots, albeit elevated, remained on a low level (Figure 10). Furthermore, no Zn-MTP was induced in Fe-deficient roots (Figure 11). Since neither BvMTP1 (the closest relative of AtMTP3), nor any other BvMTP of the Zn-subgroup is located in the tonoplast (Supporting Information: Figure S7), MTP-mediated vacuolar Zn sequestration may not exist in sugar beet. However, vacuolar localization of BvMTP1 upon heterologous expression in Arabidopsis (Figure 4) suggests that this transporter may reach the tonoplast under specific conditions. The mechanistic basis of the limited Zn uptake by Fe-deficient sugar beet is unclear and may be due to a higher selectivity of the sugar beet Fe acquisition system. This notion is supported by the finding that high Zn load did not suppress Fe uptake in sugar beet (Figure 12 and Sagardoy et al., 2009), which is in contrast to a negative impact in Arabidopsis (Lešková et al., 2017). Yeast complementation experiments indicated that BvIRT1 also transports Zn like its Arabidopsis counterpart (Supporting Information: Figure S15). The lower Zn accumulation is thus unlikely to be based on the selectivity of BvIRT1. An alternative mechanism may lie in the release of flavins by roots of sugar beet, but not Arabidopsis (Sisó-Terraza et al., 2016). These act as redox shuttles, increasing the efficiency of Fe (III) reduction. In consequence, flavins may rise the ratio of Fe^{2+} to competing divalent cations for uptake by IRT1. In line with this, the removal of flavins decreased Fe acquisition, but increased the accumulation of Zn and Mn by Fe-deficient sugar beet (Sisó-Terraza et al., 2016).

Such a selectivity mechanism of the sugar beet Fe acquisition machinery would not be specific for Zn, but extend to other secondary IRT1 substrates. In Arabidopsis, Mn concentrations are tremendously increased under Fe deficiency, in particular in roots, where 15- to 25-fold higher levels have been reported (Eroglu et al., 2016; Vert et al., 2002), whereas in shoots, Mn concentrations are increased less drastically by two- to threefold (Eroglu et al., 2016; Lešková et al., 2017). The strong accumulation of Mn in vacuoles of Fe-deficient roots is primarily mediated by AtMTP8 (Eroglu et al., 2016), which is amongst the most strongly upregulated genes upon Fe deficiency in Arabidopsis (Yang et al., 2010), also under the conditions of this study (Supporting Information: Figure S13). AtMTP8 is essential to avoid Fe chlorosis in the presence of Mn, most likely by preventing an inhibition of the ferric chelate reductase by Mn (Eroglu et al., 2016). In sugar beet, Fe deficiency provoked an increase in shoot and root Mn concentrations (Figure 10), but the latter was much less pronounced than found in Arabidopsis. In another study, Fe deficiency even did not induce any Mn accumulation in sugar beet roots (Sisó-Terraza et al., 2016). This lower Mn accumulation was paralleled by the surprising absence of transcriptional activation of *BvMTP8.1*, in roots, the vacuolar homolog of *AtMTP8* (Figure 11). The second vacuolar Mn/Fe-MTP identified in this study, *BvMTP11α*, was also unresponsive to Fe deficiency. Hence, MTP-mediated sequestration of Mn in root vacuoles is not part of the Fe deficiency response in sugar beet. The mechanism of Mn accumulation in sugar beet, alike that of the residual Mn accumulation Arabidopsis *mtp8* mutants (Eroglu et al., 2016), is unresolved. It may rely on the constitutively expressed Mn/Fe-MTPs, which may be regulated on a posttranslational level by phosphorylation, as was described recently for AtMTP8 (Zhang et al., 2021). Alternatively, Mn may be accumulated in other compartments, for example by the endomembrane-localized BvMTP8.2, which is induced in Fe-deficient sugar beet leaves (Figure 11). Owing to its

capability for Fe transport (Figure 2), a role of BvMTP8.2 in Fe handling can also not be excluded, as hypothesized above for Mn-deficient roots.

High Mn and Zn load have been shown to reduce Fe uptake and to induce the Fe deficiency response in Arabidopsis, including the upregulation of *AtMTP8* and *AtIRT1* in a FIT-dependent manner (Eroglu et al., 2016). In sugar beet, no vacuolar Mn/Fe-MTP was transcriptionally induced by high Mn (Figure 12), reflecting the situation under Fe deficiency. This was tremendously different under high Zn load, where members of the Zn-MTP family (*BvMTP1*, *4*, and *5*) were upregulated extraordinarily in roots and leaves (Figure 12). This response is in stark contrast to Arabidopsis and poplar, where Zn-MTP transporters are not transcriptionally regulated by Zn excess (Blaudez et al., 2003; Dräger et al., 2004; van der Zaal et al., 1999). The activation of BvMTP1 by Zn overload, but not by Fe deficiency, points to its regulation by Zn rather than by Zn-induced Fe deficiency.

Intriguingly, despite the competition by Mn or Zn, Fe accumulation was not hampered, but promoted in roots of high-Mn and high-Zn media (Figure 12). The observed upregulation of *BvIRT1* by Mn or Zn excess was unlikely to have mediated this effect alone, since Zn or Mn accumulation, respectively, were not increased. Similar to Fe deficiency, a high competitiveness of Fe for uptake, presumably mediated by exudated flavins, may have been instrumental for this Fe accumulation.

Taken together, this study, which combined an analysis of the MTP family and responses to transition metal imbalances in sugar beet, has revealed a number of surprising insights. It identified a chloroplast-localized MTP protein and pointed to a role of alternative splicing in determining the localization and substrate selectivity of the transporters. Most importantly, it relativizes current models of metal homeostasis. Neither ER-tunneling-based Zn translocation, nor Zn and Mn sequestration by FIT-dependent *MTP* activation are conserved between Arabidopsis and sugar beet. Conversely, sugar beet displays a strong transcriptional activation of *MTP*s by Zn toxicity not found in Arabidopsis. This limited generalizability of Arabidopsis-based metal homeostasis concepts calls for further mechanistic studies on nonmodel species to uncover the phylogenetic diversity of metal homeostasis networks. A crop-specific understanding of metal handling will also be fundamental for crop improvement strategies.

ACKNOWLEDGMENTS

We thank Anja Janssen and Tina Peiter-Volk for skillful plant husbandry and excellent technical support, Stefanie Höller for assistance with microscopy, Ahmad H. Kabir and Johannes Schneider for preliminary experiments, and Stephan Clemens (University of Bayreuth) for providing seeds of the Arabidopsis *ozs1* mutant. Seeds of the sugar beet line KWS2320 were kindly provided by KWS Saat SE (Einbeck, Germany); we thank Britta Schulz for the supply of the material. This work was supported by the European Regional Development Fund (ERDF) within the State Research Focus Program "Molecular Biosciences as a Motor for a Knowledge-Based Economy" (ZS/2016/06/79740 to E.P.), by the European Social Fund (ESF) within the AGRIPOLY graduate school (ZS/2016/08/80644 to E.P.), and by the German Research Foundation (DFG, grant INST271/371-1 FUGG to Ingo Heilmann). Open Access funding enabled and organized by Projekt DEAL.

CONFLICT OF INTEREST STATEMENT

The authors declare no conflict of interest.

DATA AVAILABILITY STATEMENT

Sequence data of sugar beet genes can be found in the GenBank database under the following accession numbers: BvMTP1 (XM_010690275.2), BvMTP4 (XM_019251003.1), BvMTP5 (XM_010674342.2), BvMTP6 (XM_010686101.2), BvMTP7α/β (XM_010697785.2), BvMTP 8.1 (XM_010695567.2), BvMTP8.2 (XM_010675225.2), BvMTP9α (XM_010694258.2), BvMTP9β (XM_010694257.2), BvMTP11α (XM_010671512.2), BvMTP11β (XM_010671513.2), and BvMTP12 (XM_010672890.2), BvIRT1 (XM_010688202.1), BvIRT2 (XM_010674870.1), BvIRT3 (XM_010668958.2), BvFER1 (XM_010694635.2), BvFIT1 (XM_010690858.2).

ORCID

Edgar Peiter http://orcid.org/0000-0002-9104-3238

REFERENCES

Agorio, A., Giraudat, J., Bianchi, M.W., Marion, J., Espagne, C., Castaings, L. et al. (2017) Phosphatidylinositol 3-phosphate-binding protein AtPH1 controls the localization of the metal transporter NRAMP1 in *Arabidopsis*. *Proceedings of the National Academy of Sciences of the United States of America*, 114, E3354–E3363.

Alejandro, S., Höller, S., Meier, B. & Peiter, E. (2020) Manganese in plants: from acquisition to subcellular allocation. *Frontiers in Plant Science*, 11, 300.

Alloway, B.J. (2009) Soil factors associated with zinc deficiency in crops and humans. *Environmental Geochemistry and Health*, 31, 537–548.

Andresen, E., Peiter, E. & Küpper, H. (2018) Trace metal metabolism in plants. *Journal of Experimental Botany*, 69, 909–954.

Arrivault, S., Senger, T. & Krämer, U. (2006) The Arabidopsis metal tolerance protein AtMTP3 maintains metal homeostasis by mediating Zn exclusion from the shoot under Fe deficiency and Zn oversupply. *The Plant Journal*, 46, 861–879.

Baker, N.R. (2008) Chlorophyll fluorescence: A probe of photosynthesis in vivo. *Annual Review of Plant Biology*, 59, 89–113.

Barberon, M. & Geldner, N. (2014) Radial transport of nutrients: the plant root as a polarized epithelium. *Plant Physiology*, 166, 528–537.

Blaudez, D., Kohler, A., Martin, F., Sanders, D. & Chalot, M. (2003) Poplar metal tolerance protein 1 confers zinc tolerance and is an oligomeric vacuolar zinc transporter with an essential leucine zipper motif. *The Plant Cell*, 15, 2911–2928.

Briat, J.-F., Dubos, C. & Gaymard, F. (2015) Iron nutrition, biomass production, and plant product quality. *Trends in Plant Science*, 20, 33–40.

Cailliatte, R., Lapeyre, B., Briat, J.F., Mari, S. & Curie, C. (2009) The NRAMP6 metal transporter contributes to cadmium toxicity. *Biochemical Journal*, 422, 217–228.

Cailliatte, R., Schikora, A., Briat, J.F., Mari, S. & Curie, C. (2010) High-affinity manganese uptake by the metal transporter NRAMP1 is

essential for *Arabidopsis* growth in low manganese conditions. *The Plant Cell*, 22, 904–917.

Cakmak, I. (2000) Tansley review no. 111: possible roles of zinc in protecting plant cells from damage by reactive oxygen species. *New Phytologist*, 146, 185–205.

Chen, Z., Fujii, Y., Yamaji, N., Masuda, S., Takemoto, Y., Kamiya, T. et al. (2013) Mn tolerance in rice is mediated by MTP8.1, a member of the cation diffusion facilitator family. *Journal of Experimental Botany*, 64, 4375–4387.

Chu, H.-H., Car, S., Socha, A.L., Hindt, M.N., Punshon, T. & Guerinot, M.L. (2017) The Arabidopsis MTP8 transporter determines the localization of manganese and iron in seeds. *Scientific Reports*, 7, 11024.

Clough, S.J. & Bent, A.F. (1998) Floral dip: a simplified method for *Agrobacterium*-mediated transformation of *Arabidopsis thaliana*. *The Plant Journal*, 16, 735–743.

Colombo, C., Palumbo, G., He, J.-Z., Pinton, R. & Cesco, S. (2014) Review on iron availability in soil: interaction of Fe minerals, plants, and microbes. *Journal of Soils and Sediments*, 14, 538–548.

Corpas, F.J., Barroso, J.B., Palma, J.M. & Rodriguez-Ruiz, M. (2017) Plant peroxisomes: A nitro-oxidative cocktail. *Redox Biology*, 11, 535–542.

Delhaize, E., Gruber, B.D., Pittman, J.K., White, R.G., Leung, H., Miao, Y. et al. (2007) A role for the *AtMTP11* gene of Arabidopsis in manganese transport and tolerance. *The Plant Journal*, 51, 198–210.

Desbrosses-Fonrouge, A.-G., Voigt, K., Schröder, A., Arrivault, S., Thomine, S. & Krämer, U. (2005) *Arabidopsis thaliana* MTP1 is a Zn transporter in the vacuolar membrane which mediates Zn detoxification and drives leaf Zn accumulation. *FEBS Letters*, 579, 4165–4174.

Dohm, J.C., Minoche, A.E., Holtgräwe, D., Capella-Gutiérrez, S., Zakrzewski, F., Tafer, H. et al. (2014) The genome of the recently domesticated crop plant sugar beet (*Beta vulgaris*). *Nature*, 505, 546–549.

Dong, C., He, F., Berkowitz, O., Liu, J., Cao, P., Tang, M. et al. (2018) Alternative splicing plays a critical role in maintaining mineral nutrient homeostasis in rice *(Oryza sativa)*. *The Plant Cell*, 30, 2267–2285.

Dräger, D.B., Desbrosses-Fonrouge, A.-G., Krach, C., Chardonnens, A.N., Meyer, R.C., Saumitou-Laprade, P. et al. (2004) Two genes encoding *Arabidopsis halleri* MTP1 metal transport proteins co-segregate with zinc tolerance and account for high *MTP1* transcript levels. *The Plant Journal*, 39, 425–439.

Draycott, A.P. (2006) *Sugar beet*. Oxford: Blackwell.

Erbasol, I., Bozdag, G.O., Koc, A., Pedas, P. & Karakaya, H.C. (2013) Characterization of two genes encoding metal tolerance proteins from *Beta vulgaris* subspecies *maritima* that confers manganese tolerance in yeast. *BioMetals*, 26, 795–804.

Eroglu, S., Giehl, R.F.H., Meier, B., Takahashi, M., Terada, Y., Ignatyev, K. et al. (2017) Metal tolerance protein 8 mediates manganese homeostasis and iron re-allocation during seed development and germination. *Plant Physiology*, 174, 1633–1647.

Eroglu, S., Meier, B., von Wirén, N. & Peiter, E. (2016) The vacuolar manganese transporter MTP8 determines tolerance to iron deficiency-induced chlorosis in Arabidopsis. *Plant Physiology*, 170, 1030–1045.

Farthing, E.C., Menguer, P.K., Fett, J.P. & Williams, L.E. (2017) OsMTP11 is localised at the Golgi and contributes to Mn tolerance. *Scientific Reports*, 7, 15258.

Filichkin, S., Priest, H.D., Megraw, M. & Mockler, T.C. (2015) Alternative splicing in plants: directing traffic at the crossroads of adaptation and environmental stress. *Current Opinion in Plant Biology*, 24, 125–135.

Fu, X.-Z., Tong, Y.-H., Zhou, X., Ling, L.-L., Chun, C.-P., Cao, L. et al. (2017) Genome-wide identification of sweet Orange *(Citrus sinensis)* metal tolerance proteins and analysis of their expression patterns under zinc, manganese, copper, and cadmium toxicity. *Gene*, 629, 1–8.

Fujiwara, T., Kawachi, M., Sato, Y., Mori, H., Kutsuna, N., Hasezawa, S. et al. (2015) A high molecular mass zinc transporter MTP12 forms a functional heteromeric complex with MTP5 in the Golgi in *Arabidopsis thaliana*. *FEBS Journal*, 282, 1965–1979.

Gollhofer, J., Timofeev, R., Lan, P., Schmidt, W. & Buckhout, T.J. (2014) Vacuolar-iron-transporter1-like proteins mediate iron homeostasis in Arabidopsis. *PLoS One*, 9, e110468.

Gustin, J.L., Zanis, M.J. & Salt, D.E. (2011) Structure and evolution of the plant cation diffusion facilitator family of ion transporters. *BMC Evolutionary Biology*, 11, 76.

He, J., Rössner, N., Hoang, M.T.T., Alejandro, S. & Peiter, E. (2021) Transport, functions, and interaction of calcium and manganese in plant organellar compartments. *Plant Physiology*, 187, 1940–1972.

He, J., Yang, B., Hause, G., Rössner, N., Peiter-Volk, T., Schattat, M.H. et al. (2022) The trans-Golgi-localized protein BICAT3 regulates manganese allocation and matrix polysaccharide biosynthesis. *Plant Physiology*, 190, 2579–2600.

Hebbern, C.A., Laursen, K.H., Ladegaard, A.H., Schmidt, S.B., Pedas, P., Bruhn, D. et al. (2009) Latent manganese deficiency increases transpiration in barley (*Hordeum vulgare*). *Physiologia Plantarum*, 135, 307–316.

Höller, S., Küpper, H., Brückner, D., Garrevoet, J., Spiers, K., Falkenberg, G. et al. (2022) Overexpression of *metal tolerance protein 8* reveals new aspects of metal transport in *Arabidopsis thaliana* seeds. *Plant Biology*, 24, 23–29.

Hou, L., Gu, D., Li, Y., Li, J., Li, J., Chen, X. et al. (2019) Phylogenetic and expression analysis of Mn-CDF transporters in pear (*Pyrus bretschneideri* Rehd.). *Plant Molecular Biology Reporter*, 37, 98–110.

Kobae, Y., Uemura, T., Sato, M.H., Ohnishi, M., Mimura, T., Nakagawa, T. et al. (2004) Zinc transporter of *Arabidopsis thaliana* AtMTP1 is localized to vacuolar membranes and implicated in zinc homeostasis. *Plant and Cell Physiology*, 45, 1749–1758.

Kolaj-Robin, O., Russell, D., Hayes, K.A., Pembroke, J.T. & Soulimane, T. (2015) Cation diffusion facilitator family: structure and function. *FEBS Letters*, 589, 1283–1295.

Komarova, N.Y., Meier, S., Meier, A., Grotemeyer, M.S. & Rentsch, D. (2012) Determinants for *Arabidopsis* peptide transporter targeting to the tonoplast or plasma membrane. *Traffic*, 13, 1090–1105.

Lanquar, V., Ramos, M.S., Lelièvre, F., Barbier-Brygoo, H., Krieger-Liszkay, A., Krämer, U. et al. (2010) Export of vacuolar manganese by AtNRAMP3 and AtNRAMP4 is required for optimal photosynthesis and growth under manganese deficiency. *Plant Physiology*, 152, 1986–1999.

Lešková, A., Giehl, R.F.H., Hartmann, A., Fargašová, A. & von Wirén, N. (2017) Heavy metals induce iron-deficiency responses at different hierarchic and regulatory levels. *Plant Physiology*, 174, 1648–1668.

Lin, Y.-F., Liang, H.-M., Yang, S.-Y., Boch, A., Clemens, S., Chen, C.-C. et al. (2009) Arabidopsis IRT3 is a zinc-regulated and plasma membrane localized zinc/iron transporter. *New Phytologist*, 182, 392–404.

Ma, G., Li, J., Li, J., Li, Y., Gu, D., Chen, C. et al. (2018) OsMTP11, a trans-Golgi network localized transporter, is involved in manganese tolerance in rice. *Plant Science*, 274, 59–69.

Mager, S., Schönberger, B. & Ludewig, U. (2018) The transcriptome of zinc deficient maize roots and its relationship to DNA methylation loss. *BMC Plant Biology*, 18, 372.

Maillard, A., Diquãlou, S., Billard, V., Laine, P., Garnica, M., Prudent, M. et al. (2015) Leaf mineral nutrient remobilization during leaf senescence and modulation by nutrient deficiency. *Frontiers in Plant Science*, 6, 317.

Menguer, P.K., Farthing, E., Peaston, K.A., Ricachenevsky, F.K., Fett, J.P. & Williams, L.E. (2013) Functional analysis of the rice vacuolar zinc transporter OsMTP1. *Journal of Experimental Botany*, 64, 2871–2883.

Montanini, B., Blaudez, D., Jeandroz, S., Sanders, D. & Chalot, M. (2007) Phylogenetic and functional analysis of the cation diffusion

facilitator (CDF) family: improved signature and prediction of substrate specificity. *BMC Genomics*, 8, 107.
Monteiro, F., Frese, L., Castro, S., Duarte, M.C., Paulo, O.S., Loureiro, J. et al. (2018) Genetic and genomic tools to asssist sugar beet improvement: the value of the crop wild relatives. *Frontiers in Plant Science*, 9, 74.
Müdsam, C., Wollschläger, P., Sauer, N. & Schneider, S. (2018) Sorting of *Arabidopsis* NRAMP3 and NRAMP4 depends on adaptor protein complex AP4 and a dileucine-based motif. *Traffic*, 19, 503–521.
Nelson, B.K., Cai, X. & Nebenführ, A. (2007) A multicolored set of in *vivo* organelle markers for co-localization studies in Arabidopsis and other plants. *The Plant Journal*, 51, 1126–1136.
Nour-Eldin, H.H., Hansen, B.G., Nørholm, M.H.H., Jensen, J.K. & Halkier, B.A. (2006) Advancing uracil-excision based cloning towards an ideal technique for cloning PCR fragments. *Nucleic Acids Research*, 34, e122.
Olt, P., Alejandro-Martinez, S., Fermum, J., Ramos, E., Peiter, E. & Ludewig, U. (2022) The vacuolar transporter LaMTP8.1 detoxifies manganese in leaves of *Lupinus albus*. *Physiologia Plantarum*, 174, e13807.
Pedas, P., Schiller Stokholm, M., Hegelund, J.N., Ladegård, A.H., Schjoerring, J.K. & Husted, S. (2014) Golgi localized barley *MTP8* proteins facilitate Mn transport. *PLoS One*, 9, e113759.
Peiter, E., Montanini, B., Gobert, A., Pedas, P., Husted, S., Maathuis, F.J.M. et al. (2007) A secretory pathway-localized cation diffusion facilitator confers plant manganese tolerance. *Proceedings of the National Academy of Sciences of the United States of America*, 104, 8532–8537.
Pottier, M., Dumont, J., Masclaux-Daubresse, C. & Thomine, S. (2019) Autophagy is essential for optimal translocation of iron to seeds in Arabidopsis. *Journal of Experimental Botany*, 70, 859–869.
Ram, H., Kaur, A., Gandass, N., Singh, S., Deshmukh, R., Sonah, H. et al. (2019) Molecular characterization and expression dynamics of MTP genes under various spatio-temporal stages and metal stress conditions in rice. *PLoS One*, 14, e0217360.
Ricachenevsky, F.K., Menguer, P.K., Sperotto, R.A., Williams, L.E. & Fett, J.P. (2013) Roles of plant metal tolerance proteins (MTP) in metal storage and potential use in biofortification strategies. *Frontiers in Plant Science*, 4, 144.
Rodríguez-Celma, J., Tsai, Y.-H., Wen, T.-N., Wu, Y.-C., Curie, C. & Schmidt, W. (2016) Systems-wide analysis of manganese deficiency-induced changes in gene activity of *Arabidopsis* roots. *Scientific Reports*, 6, 35846.
Sagardoy, R., Morales, F., López-Millán, A.-F., Abadía, A. & Abadía, J. (2009) Effects of zinc toxicity on sugar beet (*Beta vulgaris* L.) plants grown in hydroponics. *Plant Biology*, 11, 339–350.
Schmidt, S.B., Jensen, P.E. & Husted, S. (2016) Manganese deficiency in plants: the impact on photosystem II. *Trends in Plant Science*, 21, 622–632.
Schmidt, S.B., Pedas, P., Laursen, K.H., Schjoerring, J.K. & Husted, S. (2013) Latent manganese deficiency in barley can be diagnosed and remediated on the basis of chlorophyll *a* fluorescence measurements. *Plant and Soil*, 372, 417–429.
Schwarz, B. & Bauer, P. (2020) FIT, a regulatory hub for iron deficiency and stress signaling in roots, and FIT-dependent and -independent gene signatures. *Journal of Experimental Botany*, 71, 1694–1705.
Shanmugam, V., Lo, J.-C., Wu, C.-L., Wang, S.-L., Lai, C.-C., Connolly, E.L. et al. (2011) Differential expression and regulation of iron-regulated metal transporters in *Arabidopsis halleri* and *Arabidopsis thaliana*—the role in zinc tolerance. *New Phytologist*, 190, 125–137.
Shirazi, Z., Abedi, A., Kordrostami, M., Burritt, D.J. & Hossain, M.A. (2019) Genome-wide identification and characterization of the metal tolerance protein (MTP) family in grape (*Vitis vinifera* L.). *3 Biotech*, 9, 199.
Sinclair, S.A., Senger, T., Talke, I.N., Cobbett, C.S., Haydon, M.J. & Krämer, U. (2018) Systemic upregulation of MTP2- and HMA2-mediated Zn partitioning to the shoot supplements local Zn deficiency responses. *The Plant Cell*, 30, 2463–2479.
Sisó-Terraza, P., Rios, J.J., Abadía, J., Abadía, A. & Álvarez-Fernández, A. (2016) Flavins secreted by roots of iron-deficient *Beta vulgaris* enable mining of ferric oxide via reductive mechanisms. *New Phytologist*, 209, 733–745.
Takemoto, Y., Tsunemitsu, Y., Fujii-Kashino, M., Mitani-Ueno, N., Yamaji, N., Ma, J.F. et al. (2017) The tonoplast-localized transporter MTP8.2 contributes to manganese detoxification in the shoots and roots of *Oryza sativa* L. *Plant and Cell Physiology*, 58, 1573–1582.
Ueno, D., Sasaki, A., Yamaji, N., Miyaji, T., Fujii, Y., Takemoto, Y. et al. (2015) A polarly localized transporter for efficient manganese uptake in rice. *Nature Plants*, 1, 15170.
van de Mortel, J.E., Almar Villanueva, L., Schat, H., Kwekkeboom, J., Coughlan, S., Moerland, P.D. et al. (2006) Large expression differences in genes for iron and zinc homeostasis, stress response, and lignin biosynthesis distinguish roots of *Arabidopsis thaliana* and the related metal hyperaccumulator *Thlaspi caerulescens*. *Plant Physiology*, 142, 1127–1147.
van der Zaal, B.J., Neuteboom, L.W., Pinas, J.E., Chardonnens, A.N., Schat, H., Verkleij, J.A.C. et al. (1999) Overexpression of a novel Arabidopsis gene related to putative zinc-transporter genes from animals can lead to enhanced zinc resistance and accumulation. *Plant Physiology*, 119, 1047–1056.
Vatansever, R., Filiz, E. & Eroglu, S. (2017) Genome-wide exploration of metal tolerance protein (*MTP*) genes in common wheat (*Triticum aestivum*): insights into metal homeostasis and biofortification. *BioMetals*, 30, 217–235.
Vert, G., Grotz, N., Dédaldéchamp, F., Gaymard, F., Guerinot, M.L., Briat, J.-F. et al. (2002) IRT1, an Arabidopsis transporter essential for iron uptake from the soil and for plant growth. *The Plant Cell*, 14, 1223–1233.
Weber, M., Deinlein, U., Fischer, S., Rogowski, M., Geimer, S., Tenhaken, R. et al. (2013) A mutation in the *Arabidopsis thaliana* cell wall biosynthesis gene *pectin methylesterase 3* as well as its aberrant expression cause hypersensitivity specifically to Zn. *The Plant Journal*, 76, 151–164.
Yang, T.J.W., Perry, P.J., Ciani, S., Pandian, S. & Schmidt, W. (2008) Manganese deficiency alters the patterning and development of root hairs in *Arabidopsis*. *Journal of Experimental Botany*, 59, 3453–3464.
Yang, T.J.W., Lin, W.-D. & Schmidt, W. (2010) Transcriptional profiling of the Arabidopsis iron deficiency response reveals conserved transition metal homeostasis networks. *Plant Physiology*, 152, 2130–2141.
Yruela, I. (2013) Transition metals in plant photosynthesis. *Metallomics*, 5, 1090–1109.
Zhang, Z., Fu, D., Sun, Z., Ju, C., Miao, C., Wang, Z. et al. (2021) Tonoplast-associated calcium signaling regulates manganese homeostasis in Arabidopsis. *Molecular Plant*, 14, 805–819.

SUPPORTING INFORMATION

Additional supporting information can be found online in the Supporting Information section at the end of this article.

How to cite this article: Alejandro, S., Meier, B., Hoang, M.T.T. & Peiter, E. (2023) Cation Diffusion Facilitator proteins of *Beta vulgaris* reveal diversity of metal handling in dicotyledons. *Plant, Cell & Environment*, 46, 1629–1652. https://doi.org/10.1111/pce.14544